

On the stability of the unsmoothed Fourier method for hyperbolic equations

Jonathan Goodman¹, Thomas Hou¹, and Eitan Tadmor²

¹ Courant Institute of Mathematical Sciences, New-York University, New-York, NY 10012, USA

² School of Mathematical Sciences, Tel-Aviv University, Tel-Aviv 69978, Israel

Received December 14, 1992/Revised version received March 1, 1993

Summary. It has been a long open question whether the pseudospectral Fourier method without smoothing is stable for hyperbolic equations with variable coefficients that change signs. In this work we answer this question with a detailed stability analysis of prototype cases of the Fourier method. We show that due to weighted L^2 -stability, the N -degree Fourier solution is *algebraically stable* in the sense that its L^2 amplification does not exceed $O(N)$. Yet, the Fourier method is *weakly L^2 -unstable* in the sense that it does experience such $O(N)$ amplification. The exact mechanism of this weak instability is due the aliasing phenomenon, which is responsible for an $O(N)$ amplification of the Fourier modes at the boundaries of the computed spectrum.

Two practical conclusions emerge from our discussion. First, the Fourier method is required to have sufficiently many modes in order to resolve the underlying phenomenon. Otherwise, the lack of *resolution* will excite the weak instability which will propagate from the slowly decaying high modes to the lower ones. Second – independent of whether smoothing was used or not, the small scale information contained in the highest modes of the Fourier solution will be destroyed by their $O(N)$ amplification. Happily, with enough resolution nothing worse can happen.

Mathematics Subject Classification (1991): 65M12

1. Introduction

In this paper we address a long open question regarding the stability of the pseudospectral Fourier method for linear hyperbolic problems with variable coefficients,

$$\frac{\partial}{\partial t} u(x, t) = \frac{\partial}{\partial x} (q(x)u(x, t)), \quad t \geq 0, x \in T[0, 2\pi).$$

The answer of this stability question is known to be affirmative for one-signed $q(x)$'s: the solution operator in this case is similar to a unitary one, which in turn implies the *weighted L^2 -stability* of the Fourier method. Our main thrust is therefore geared

Correspondence to: E. Tadmor

towards the more intriguing cases with $q(x)$'s which may change sign. Of course, the canonical stability question in this context is posed within the L^2 -setup. For partial list of references on this subject we refer to the pioneering papers of Kreiss and Olinger [KO1] and Orszag [Or1],[Or2], the early results of Fornberg [Fo], the short reviews of e.g., Gottlieb and Turkel [GTu] and Tadmor [Ta4], and to the comprehensive texts of Gottlieb and Orszag [GO], Canuto et. al. [CHQZ], Boyd [B] and Funaro [Fu].

We provide sharp estimates for the L^2 -growth of the Fourier approximation. It is shown that the N -degree Fourier approximation may be amplified – relative to its initial L^2 -size at $t = 0$, by at most a factor of order $O(N)$. In short, this says that the Fourier method is *weakly* L^2 -unstable, though this statement does not 'faithfully' explain the behavior of the Fourier method. Indeed, such dissipation-free weak instabilities are expected to turn into the easily detectable *exponential* instabilities in the presence of low-order terms, etc. [RM, Sect. 5.2]. The Fourier method, however, does not experience such exponential behavior, which partly explains why this stability question remained inconclusive in the past. We provide a rather complete description of the behavior of the Fourier method, which explains among other things how the Fourier method maintains its *algebraic* L^2 -stability in the presence of low-order perturbations, etc. Let us briefly review our main results.

That the L^2 -amplification is not larger than $O(N)$ is a consequence of the *weighted* L^2 -stability of the Fourier method stated in Sect. 2. This weighted L^2 -stability is due to the fact that as in the one-signed case, the solution operator of the Fourier method is similar to a unitary one. However, the similarity transformation in this case involves the ill-conditioned $N \times N$ Jordan blocks; as the condition number of the latter may grow linearly with N , we conclude, in Sect. 3, that there is an $O(N)$ upper-bound on the L^2 -growth. That the amplification is not smaller than $O(N)$ in certain cases is a consequence of the aliasing phenomena. In Sect. 3 we show that the aliasing relations are responsible for the $O(N)$ reflection of the Fourier modes at the boundaries of the computed spectrum. As long as the computed solution remains sufficiently smooth, this $O(N)$ amplification applies to the relatively small Fourier modes at the end of the spectrum, and therefore will not affect the L^2 -size of the overall computed solution. Yet, for nonsmooth data (– our specific example consists of L^2 delta-like initial dipole), this mechanism of high-frequency amplification will yield an L^2 -growth of order $O(N)$.

The two ingredients of weighted L^2 -stability and linear high-frequency amplification are utilized in Sect. 4 to shed further light on the behavior of the Fourier method. We first note that the changing sign(s) of $q(x)$ are responsible for the development of sharp (spatial) gradients in the underlying solution. Consequently, if the Fourier method does not contain enough modes to resolve these sharp gradients, then this will lead to the linear amplification of the rather slowly decaying high-frequency amplitudes. We conclude that independent of whether the initial conditions are smooth or not, the lack of resolution in later time will manifest itself as a weak L^2 -instability propagating from high to lower modes. We also show that whether the weak L^2 -instability is 'genuine' or is just due to lack of resolution, the *weighted* L^2 -stability guarantee that nothing worse than the $O(N)$ amplification will be excited. In particular, one concludes with the usual spectral convergence rate estimates.

We have made a serious effort to simplify the presentation of this material which otherwise involves tedious algebraic manipulations. For this reason the paper is organized as follows. In the first three sections, Sects. 2–4, we prefer to concentrate on (what is later justified to be) the prototype case of a simple 1-wave coefficient, $q(x) = \sin(x)$. The highlights of these sections include the following.

- Section 2 is devoted to the weighted L^2 -stability of the Fourier method. The main result of this section, stated in Theorem 2.1, asserts that there exists a positive definite H -weighted norm, $\|\cdot\|_H$, such that the Fourier approximation of the 1-wave equation, $u_N(\cdot, t)$, satisfies,

$$\|u_N(\cdot, t)\|_H \leq C(t)\|u_N(\cdot, 0)\|_H.$$

- Section 3 deals with the algebraically weak L^2 -instability of the Fourier method. The main result of this section, stated in Theorem 3.1, asserts that

$$C_1(t)N \leq \sup_{u_N(0) \neq 0} \frac{\|u_N(t)\|}{\|u_N(0)\|} \leq C_2(t)N.$$

- Section 4 concludes with the convergence rate estimate stated in Theorem 4.1:

$$\|u_N(\cdot, t) - u(\cdot, t)\|_{W^s} \leq \text{Const}_{s,\alpha} N^{2-\alpha} \|u(\cdot, 0)\|_{W^{s+\alpha}}, \quad \forall s + \alpha > \frac{1}{2}.$$

In Sect. 5 we turn to show that the basic ingredients introduced in Sects. 2–4 carry over to more general situations. In particular, Theorem 5.2 extends the basic weighted L^2 -stability result to arbitrary sinusoidal wave coefficients, $q(x) = \sin(px)$, $p \geq 1$. We also treat the Fourier approximation for combination of simple sinusoidal and cosinusoidal wave coefficients, based on both odd and even number of gridpoints. Numerical experiments are found to be in complete agreement with the details of our analysis.

Epilogue. The moral of our stability analysis is two-fold:

1. The Fourier approximation is required to have sufficiently many modes (or to use sufficiently refined grids) which will enable to *resolve* the underlying phenomena; otherwise, the lack of resolution will excite a weak high-frequencies instability.
2. There are various high-frequencies smoothing procedures which are known to enforce the stability of the Fourier method. Yet, the stability achieved in this manner is at the expense of destroying the small scale information contained in the corresponding high-frequencies. Our analysis shows that the plain, smoothing-free Fourier method suffers the same deficiency. Namely, the small scale information contained in the high-frequencies of the Fourier method (with or without enough resolution) is destroyed due to the $O(N)$ amplification of the latter. Happily, nothing worse can happen.

2. Weighted L^2 -Stability

We begin our discussion with the Fourier method based on an odd number¹ of $2N+1$ equally spaced grid points, $x_\nu := \nu \frac{2\pi}{2N+1}$, $\nu = 0, 1, \dots, 2N$. We let $\psi_N w(x)$ denote the N -degree trigonometric interpolant of $w(x)$ at these equally spaced grid points

$$(2.1a) \quad \psi_N w(x) = \sum_{k=-N}^N \hat{w}_k e^{ikx}, \quad \hat{w}_k := \frac{1}{2N+1} \sum_{\nu=0}^{2N} w(x_\nu) e^{-ikx_\nu}.$$

¹ The reason for this odd choice is explained in Remark 2 on page 113. We get even in Sect. 5.

Observe that the discrete Fourier coefficients \hat{w}_k are well-defined $\forall k \in \mathbb{Z}$ with period $2N + 1$, i.e.,

$$(2.1b) \quad \hat{w}_k = \hat{w}_{[k]}, \quad [k] \equiv k \pmod{2N + 1}, \quad \forall k \in \mathbb{Z}.$$

This reflects the *aliasing* phenomenon, where different waves in the discrete Fourier expansion are tagged by the same wave number modulo $2N + 1$.

We want to solve by Fourier method the scalar, 2π -periodic hyperbolic equation

$$(2.2) \quad \frac{\partial}{\partial t} u(x, t) = \frac{\partial}{\partial x} (q(x)u(x, t)), \quad t \geq 0, \quad x \in T[0, 2\pi).$$

To this end we approximate the interpolant of the exact solution, $\psi_N u(\cdot, t)$, using an N -trigonometric polynomial, $u_N(x, t) = \sum_{k=-N}^N \hat{u}_k(t) e^{ikx}$, which is governed by the semi-discrete Fourier approximation

$$(2.3) \quad \frac{\partial}{\partial t} u_N(x, t) = \frac{\partial}{\partial x} \psi_N [q(x)u_N(x, t)].$$

This Fourier approximation could be realized in the physical space by the $(2N + 1)$ -vector of its grid values, $u(t) = (u(x_0, t), \dots, u(x_{2N}, t))$, which is governed by the system of ODE's

$$(2.4) \quad \frac{d}{dt} u(t) = DQ u(t).$$

Here, D denotes the $(2N + 1) \times (2N + 1)$ Fourier differentiation matrix,

$$D_{jk} = \frac{(-1)^{j-k}}{2 \sin\left(\frac{x_j - x_k}{2}\right)} (1 - \delta_{jk}),$$

and Q is a diagonal matrix representing multiplication by $q(x)$, $Q_{jk} = \delta_{jk} q(x_k)$. Together with one's favorite ODE solver², this system give rise to a fully discrete, consistent (— in fact, spectrally accurate) approximation of (2.2), and we now raise the stability question of the underlying semi-discrete Fourier approximation.

The stability question has a rather simple affirmative answer in case $q(x)$ is one-signed, say positive, so that $Q > 0$. Indeed, since in this case DQ is similar to the antisymmetric matrix $\mathcal{S} = Q^{\frac{1}{2}} D Q^{\frac{1}{2}}$, it implies that the solution operator is similar to a unitary one, $e^{DQ t} = Q^{-\frac{1}{2}} U(t) Q^{\frac{1}{2}}$ with $U(t) = e^{\mathcal{S} t}$, and weighted L^2 -stability follows,

$$(2.5) \quad \|u_N(t)\|_H = \|u_N(0)\|_H, \quad H = Q > 0.$$

Observe that if $q(x)$ is bounded away from zero then H has a uniformly bounded condition number, $Const = \frac{\max q(x)}{\min q(x)} < \infty$, and hence the weighted L^2 -stability in (2.5) could be translated into the usual L^2 -stability,

$$\|u_N(t)\| \leq Const \cdot \|u_N(0)\|.$$

We now turn to consider the more intriguing case where $q(x)$ may change sign. In this section we take a rather detailed look at the prototype case of $q(x) = \sin(x)$:

² The numerical experiments reported below employ the standard 4th order Runge-Kutta ODE solver.

$$(2.6) \quad \frac{\partial}{\partial t} u_N(x, t) = \frac{\partial}{\partial x} \psi_N [\sin(x) u_N(x, t)].$$

We shall show that as in the one-signed case, the solution operator associated with (2.6) is also similar to a unitary matrix – consult (2.20) below for the precise statement. This in turn leads to the announced weighted L^2 -stability. It should be noted, however, that the similarity transformation in this case involves the ill-conditioned $N \times N$ Jordan blocks; as the condition number of the latter may grow linearly with N , this in turn implies the *weak* L^2 -instability discussed in Sect. 3.

We begin by noting that the Fourier approximation (2.6) admits a rather simple representation in the Fourier space, using the $(2N+1)$ -vector of its Fourier coefficients, $\hat{u}(t) := (\hat{u}_{-N}(t), \dots, \hat{u}_N(t))$. With the periodic extension of $\hat{u}_k(t) \forall k \in \mathbb{Z}$ in mind – consult (2.1b), we are able to express the interpolant of $\sin(x)u_N(x, t)$ as

$$\psi_N [\sin(x)u_N(x, t)] = \sum_{k=-N}^N \frac{1}{2i} [\hat{u}_{k-1}(t) - \hat{u}_{k+1}(t)] e^{ikx},$$

so that the Fourier approximation (2.6) then reads

$$(2.7a) \quad \frac{d}{dt} \hat{u}_k(t) = \frac{k}{2} [\hat{u}_{k-1}(t) - \hat{u}_{k+1}(t)], \quad -N \leq k \leq N,$$

augmented by the aliasing boundary conditions (2.1b)

$$(2.7b) \quad \hat{u}_{-(N+1)}(t) = \hat{u}_N(t) \equiv \bar{\hat{u}}_{-N}(t), \quad \hat{u}_{N+1}(t) = \hat{u}_{-N}(t) \equiv \bar{\hat{u}}_N(t).$$

Thus, in the Fourier space, our approximation is converted into the system of ODE's

$$(2.8) \quad \frac{d}{dt} \hat{u}(t) = \Lambda \hat{Q} \hat{u}(t), \quad \Lambda_{jk} = k \delta_{jk}, \quad \hat{Q} = \frac{1}{2} \begin{bmatrix} 0 & -1 & 0 & \dots & -1 \\ 1 & 0 & -1 & & 0 \\ 0 & 1 & \ddots & \ddots & \vdots \\ \vdots & & \ddots & 0 & -1 \\ -1 & 0 & \dots & 1 & 0 \end{bmatrix}.$$

Remark. We note in passing that the two representations of the Fourier approximation – the ODE system (2.4) in the real space (with $q(x_k) = \sin(x_k)$) and the ODE system (2.8) in Fourier space, are unitarily equivalent: indeed, $\Lambda \hat{Q} = \mathcal{F}^* D Q \mathcal{F}$ with \mathcal{F} being the unitary Fourier matrix,

$$\mathcal{F}_{jk} := (2N+1)^{-\frac{1}{2}} e^{ijk\Delta x}, \quad -N \leq j, k \leq N.$$

We shall study the stability of (2.6) in terms of its unitarily equivalent Fourier representation in (2.8), which is decoupled into its real and imaginary parts, $\hat{u}(t) = a(t) + ib(t)$. According to (2.7a)-(2.7b), the real part of the Fourier coefficients, $a_k(t) := \Re \hat{u}_k(t)$, satisfies

$$(2.9a) \quad \frac{d}{dt} a_k(t) = \frac{k}{2} [a_{k-1}(t) - a_{k+1}(t)], \quad -N \leq k \leq N,$$

augmented with the boundary conditions

$$(2.9b) \quad a_{-(N+1)}(t) = a_{-N}(t), \quad a_{N+1}(t) = a_N(t).$$

The imaginary part of the Fourier coefficients, $b_k(t) := \Im \hat{u}_k(t)$, satisfy the same recurrence relations as before

$$(2.10a) \quad \frac{d}{dt} b_k(t) = \frac{k}{2} [b_{k-1}(t) - b_{k+1}(t)], \quad -N \leq k \leq N,$$

the only difference lies in the augmenting boundary conditions which now read

$$(2.10b) \quad b_{-(N+1)}(t) = -b_{-N}(t), \quad b_{N+1}(t) = -b_N(t).$$

The weighted stability of the ODE systems (2.9) and (2.10) is revealed upon change of variables. For the real part in (2.9) we introduce the local differences,

$$\rho_k^-(t) := a_k(t) - a_{k+1}(t);$$

for the imaginary part in (2.10) we consider the local averages,

$$\rho_k^+(t) := b_k(t) + b_{k+1}(t).$$

Differencing consecutive terms in (2.9a) while adding consecutive terms in (2.10a) we find

$$(2.11a) \quad \frac{d}{dt} \rho_k^\pm(t) = \frac{k}{2} \rho_{k-1}^\pm(t) - \frac{k+1}{2} \rho_{k+1}^\pm(t) \pm \frac{1}{2} \rho_k^\pm(t), \quad -N \leq k \leq N-1.$$

The motivation for considering this specific change of variables stems from the side conditions in (2.9b) and (2.10b), which are now translated into zero boundary values

$$(2.11b) \quad \rho_{-(N+1)}^\pm(t) = \rho_N^\pm(t) = 0.$$

Observe that (2.11a), (2.11b) amount to a fixed translation of *antisymmetric* ODE systems for $\rho^-(t) := (\rho_{-N}^-(t), \dots, \rho_{N-1}^-(t))$ and $\rho^+(t) := (\rho_{-N}^+(t), \dots, \rho_{N-1}^+(t))$, that is, we have

$$(2.12) \quad \frac{d}{dt} \rho^\pm(t) = \frac{1}{2} (\pm I + \mathcal{S}) \rho^\pm(t),$$

where \mathcal{S} denotes the antisymmetric matrix

$$\mathcal{S} = \begin{bmatrix} 0 & N-1 & 0 & \dots \\ 1-N & 0 & \ddots & 0 \\ 0 & \ddots & \ddots & 1 \\ \vdots & 0 & -1 & 0 \end{bmatrix} \oplus \begin{bmatrix} 0 & -1 & 0 & \dots \\ 1 & 0 & \ddots & 0 \\ 0 & \ddots & \ddots & 1-N \\ \vdots & 0 & N-1 & 0 \end{bmatrix}.$$

The solution of these systems is expressed in terms of the *unitary* matrix $U(t) = e^{\frac{1}{2} \mathcal{S} t}$,

$$(2.13)_\pm \quad \rho^\pm(t) = e^{\pm t/2} U(t) \rho^\pm(0), \quad U^*(t) U(t) = I_{2N}.$$

The explicit solution given in (2.13) shows that our problem – when expressed in terms of the new variables $\rho^\pm(t)$, is clearly L^2 -stable,

$$\|\rho^\pm(t)\| = e^{\pm t/2} \|\rho^\pm(0)\|.$$

Remark. We note that this L^2 -type argument carries over for higher derivatives, that is, the W^α -norms of $\rho^\pm(t)$ remain bounded,

$$(2.14) \quad \|\rho\|_{W^\alpha} := \|A^\alpha \rho\| = \left(\sum_k |k|^{2\alpha} |\rho_k|^2 \right)^{\frac{1}{2}}, \quad A_{jk} = k\delta_{jk}.$$

Indeed, multiplication of (2.12) on the left by $|A|^\alpha$ yields

$$\frac{d}{dt} |A|^\alpha \rho^\pm(t) = \frac{1}{2} (\pm I + \mathcal{S}^{(\alpha)}) |A|^\alpha \rho^\pm(t).$$

The matrices $\mathcal{S}^{(\alpha)} = |A|^\alpha \mathcal{S} |A|^{-\alpha}$ are not antisymmetric (except for the $\alpha = 0$ case treated before),

$$\mathcal{S}_{k,j}^{(\alpha)} = \begin{cases} |k|^\alpha k / |k-1|^\alpha & j = k-1 \neq 0 \\ -|k|^\alpha (k+1) / |k+1|^{\alpha-1} & j = k+1 \neq 0; \end{cases}$$

Nevertheless, the $\mathcal{S}^{(\alpha)}$'s are not far from being antisymmetric since their real part is bounded,

$$\mathcal{S}^{(\alpha)} + \mathcal{S}^{(\alpha)t} \leq 2C_\alpha I, \quad C_\alpha \sim \alpha.$$

This implies that

$$(2.15)_\pm \quad |A|^\alpha \rho^\pm(t) = e^{\pm t/2} e^{\mathcal{S}^{(\alpha)t/2} |A|^\alpha \rho^\pm(0)}, \quad \|e^{\mathcal{S}^{(\alpha)t/2}\|} \leq e^{C_\alpha t/2},$$

and the asserted W^α -stability then follows

$$(2.16) \quad \|\rho^\pm(t)\|_{W^\alpha} \leq e^{(C_\alpha \pm 1)t/2} \|\rho^\pm(0)\|_{W^\alpha}, \quad \|\rho\|_{W^\alpha} = \|A^\alpha \rho\|.$$

We want to interpret these L^2 -type stability statements for the ρ^\pm -variables in term of the original variables – the real and imaginary parts of the system (2.8). This will be achieved in term of simple linear transformations involving the $N \times N$ Jordan blocks

$$J_\pm = \begin{bmatrix} 1 & \pm 1 & \dots & 0 \\ 0 & 1 & \ddots & \vdots \\ \vdots & & \ddots & \pm 1 \\ 0 & \dots & 0 & 1 \end{bmatrix}.$$

To this end, let us assume temporarily that the initial conditions have zero average, i.e., that

$$(2.17) \quad a_0(0) \equiv \frac{1}{2N+1} \sum_\nu u(x_\nu, 0) = 0.$$

According to (2.9a), $a_0(t)$ remains zero $\forall t$, and so will be temporarily ignored. Then, if we let

$$\tilde{a}(t) := (a_{-N}(t), \dots, a_{-1}(t), a_1(t), \dots, a_N(t))$$

denote the 'punctured' $2N$ -vector of real part associated with (2.8), it is related to the $2N$ -vector of local differences, $\rho^-(t)$, through

$$\rho^-(t) = T_- \tilde{a}(t), \quad T_- := J_- \ominus J_-^t.$$

This enables us to rewrite the solution given in (2.13)₋ as

$$(2.18) \quad T_- \tilde{a}(t) = e^{-t/2} U(t) T_- \tilde{a}(0).$$

Similarly, since $b_0(t) \equiv \mathbb{I}m \frac{1}{2N+1} \sum_{\nu} u(x_{\nu}, t) = 0$ in the real case, it will be temporarily ignored. Then, the 'punctured' $2N$ -vector of imaginary part associated with (2.8),

$$\tilde{b}(t) := (b_{-N}(t), \dots, b_{-1}(t), b_1(t), \dots, b_{N-1}(t)),$$

is related to the $2N$ -vector of local averages, $\rho^+(t)$, through

$$\rho^+(t) = T_+ \tilde{b}(t), \quad T_+ := J_+ \oplus J_+^t,$$

which enables us to rewrite the solution given in (2.13)₊ as

$$(2.19) \quad T_+ \tilde{b}(t) = e^{t/2} U(t) T_+ \tilde{b}(0).$$

The equalities (2.18) and (2.19) confirm our assertion in the beginning of this section, namely,

Assertion. The solution operator associated with the Fourier approximation, (2.6), (2.17), is similar to the unitary matrix $\tilde{U}(t) := U(t) \oplus U(t)$, in the sense that

$$(2.20) \quad \tilde{u}(t) = T^{-1} \tilde{U}(t) T \tilde{u}(0), \quad \tilde{u}(t) := e^{t/2} \tilde{a}(t) \oplus e^{-t/2} \tilde{b}(t), \quad T := T_- \oplus T_+.$$

We are now in a position to translate this similarity into an appropriate *weighted* L^2 -stability. On the left of (2.18) we have a weighted L^2 -norm of $\tilde{a}(t)$, $\|T_- \tilde{a}(t)\| \equiv \|\tilde{a}(t)\|_{T_-^t T_-}$. Also, $U(t)$ being a unitary matrix has an L^2 -norm = 1, hence the right hand side of (2.18) does not exceed, $e^{-t/2} \|T_- \tilde{a}(0)\| \equiv e^{-t/2} \|\tilde{a}(0)\|_{T_-^t T_-}$, and therefore $\tilde{a}(t) = \mathbb{R}e(\hat{u}_{-N}(t), \dots, \hat{u}_{-1}, \hat{u}_1(t), \dots, \hat{u}_N(t))$ satisfies

$$\|\tilde{a}(t)\|_{T_-^t T_-} \leq e^{-t/2} \|\tilde{a}(0)\|_{T_-^t T_-}, \quad T_-^t T_- = J_-^t J_- \oplus J_- J_-^t.$$

Expanding the last inequality by augmenting it with the zero value of $a_0(t)$ we find the weighted L^2 -stability of the real part

$$(2.21a) \quad \|a(t)\|_{H_-} \leq e^{-t/2} \|a(0)\|_{H_-}, \quad H_- = J_-^t J_- \oplus 1 \oplus J_- J_-^t.$$

Similarly, (2.19) gives us the weighted stability of the imaginary part

$$(2.21b) \quad \|b(t)\|_{H_+} \leq e^{t/2} \|b(0)\|_{H_+}, \quad H_+ = J_+^t J_+ \oplus 1 \oplus J_+ J_+^t.$$

Summarizing (2.21a) and (2.21b) we have shown

Theorem 2.1. *Consider the Fourier method (2.6) subject to initial conditions with zero mean, (2.17). Then the following weighted L^2 -stability estimate holds*

$$(2.22) \quad \|\|u_N(t)\|\|_H \leq e^{t/2} \|\|u_N(0)\|\|_H.$$

Here $\|\|u_N(t)\|\|_H$ denotes the weighted L^2 -norm

$$(2.23) \quad \|\|u_N(t)\|\|_H := \|\mathbb{R}e \hat{u}(t) \oplus \mathbb{I}m \hat{u}(t)\|_H,$$

where the weighting matrix $H := H_- \oplus H_+ > 0$ is given by

$$\begin{aligned}
 H_{\pm} &:= J_{\pm}^t J_{\pm} \oplus 1 \oplus J_{\pm} J_{\pm}^t \\
 &= \left[\begin{array}{cccc|c|cccc}
 1 & \pm 1 & & & & & & & & & \\
 \pm 1 & 2 & \pm 1 & & & & & & & & \\
 & & \ddots & \ddots & \ddots & & & & & & \\
 & & & \ddots & \ddots & \pm 1 & & & & & \\
 & & & & \pm 1 & 2 & & & & & \\
 \hline
 & & & & & & 1 & & & & \\
 & & & & & & & 2 & \pm 1 & & \\
 & & & & & & & \pm 1 & 2 & \pm 1 & \\
 & & & & & & & & \ddots & \ddots & \ddots \\
 & & & & & & & & & \ddots & \pm 1 \\
 & & & & & & & & & & \pm 1 & 1
 \end{array} \right].
 \end{aligned}$$

We close this section with three extensions of the last weighted stability result. We first note that the requirement of initial data with zero mean in Theorem 2.1 is not a restriction. Indeed, Duhammel’s principle gives us

Corollary 2.2. (Inhomogeneous terms.) *Let $u_N(t) \equiv u_N(\cdot, t)$ denote the solution of the inhomogeneous Fourier method*

$$(2.24) \quad \frac{\partial}{\partial t} u_N(x, t) = \frac{\partial}{\partial x} \psi_N [\sin(x)u_N(x, t)] + F_N(x, t).$$

Then there exists a constant, $C(t)$, such that the following weighted L^2 -stability estimate holds

$$(2.25) \quad |||u_N(t)|||_H \leq C(t) \left[|||u_N(0)|||_H + \max_{0 \leq \tau \leq t} |||F_N(\tau)|||_H \right].$$

The proof proceeds in three steps.

1. Consider first the case where both the initial and inhomogeneous data have zero mean, $\hat{u}_0(0) = 0, \hat{F}_0(t) = 0, \forall t$. In this case Theorem 2.1 applies and Duhammel’s principle shows that (2.25) holds with, say, $C(t) = 2e^{t/2}$.
2. Next we consider the case with $F_N \equiv 0$, and arbitrary initial data $u_N(\cdot, 0)$. In this case, $w_N(\cdot, t) := u_N(\cdot, t) - \hat{u}_0(0)$ satisfies the inhomogeneous Fourier approximation (2.24) with $F_N(x, t) = \hat{u}_0(t = 0) \cos(x)$. Hence step 1. applies to $w_N(\cdot, t)$, which in turn implies (2.25) for the general homogeneous problem.
3. Finally, we apply Duhammel’s principle once more to conclude with (2.25) in the general inhomogeneous case. \square

Our second corollary shows that the weighted L^2 -stability of the Fourier method is invariant under low order perturbations.

Corollary 2.3. (Low order terms.) *Let $u_N(t) \equiv u_N(\cdot, t)$ denotes the solution of the Fourier method*

$$(2.26) \quad \frac{\partial}{\partial t} u_N(x, t) = \frac{\partial}{\partial x} \psi_N [\sin(x)u_N(x, t)] + \psi_N [p(x)u_N(x, t)], \quad p \in L^\infty[0, 2\pi).$$

Then there exists a constant, $C(t)$, such that the following weighted L^2 -stability estimate holds

$$(2.27) \quad \| \|u_N(t)\| \|_H \leq C(t) \| \|u_N(0)\| \|_H.$$

For the proof we appeal to the representation of (2.26) in Fourier space, consult (2.8),

$$\frac{d}{dt} \hat{u}(t) = [\Lambda \hat{Q} + \hat{P}] \hat{u}(t), \quad \hat{P} := \mathcal{F}^* \begin{bmatrix} p(x_0) & & \\ & \ddots & \\ & & p(x_{2N}) \end{bmatrix} \mathcal{F}.$$

Here \hat{P} is the circulant matrix whose entries, $\hat{P}_{jk} = \sum_{\ell} \hat{p}_{j-k+\ell(2N+1)}$, $|j|, |k| \leq N$, represent multiplication by $p(x)$ as a convolution in the Fourier space. Corollary 2.2 tells us that

$$\|e^{\Lambda \hat{Q} t}\|_H \leq C(t),$$

and hence by Kreiss-Strang perturbation Theorem, [RM, Sect. 3.9], we conclude that $\|e^{[\Lambda \hat{Q} + \hat{P}] t}\|_H$ is bounded in terms of $\|\hat{P}\|_H$. The latter involves the H_{\pm} -weighted norms of the real and imaginary parts of \hat{P} . The following upper bound of the real part, $\hat{c}_{k-j} = \sum_{\ell} \mathbb{R}e \hat{p}_{j-k+\ell(2N+1)}$ demonstrates the general case.

Let $w = a + ib$ denote an arbitrary $2N + 1$ -vector satisfying the aliasing relations (2.1b). Then we have

$$\frac{\|\mathbb{R}e \hat{P} a\|_{H_-}^2}{\|a\|_{H_-}^2} = \frac{\sum_{k=-N}^{N-1} \left| \sum_{j=-N}^N [\hat{c}_{k+1-j} - \hat{c}_{k-j}] a_j \right|^2}{\sum_{k=-N}^{N-1} |a_{k+1} - a_k|^2}.$$

The last quantity equals

$$\frac{\sum_{k=-N}^N \left| \sum_{j=-N}^{N-1} \hat{c}_{k-j} \Delta a_j \right|^2}{\sum_{k=-N}^N |\Delta a_k|^2}, \quad \Delta a_k := \begin{cases} a_{k+1} - a_k, & k \leq N-1 \\ 0, & k = N, \end{cases}$$

and by Parseval identity it does not exceed

$$\frac{\sum_{k=-N}^N |p(x_k) \Delta \check{a}_k|^2}{\sum_{k=-N}^N |\Delta \check{a}_k|^2} \leq \|p(\cdot)\|_{L^\infty}^2, \quad \Delta \check{a} := \mathcal{F} \Delta a.$$

A similar treatment applies to the other terms.

For an alternative proof one can argue along the lines of Theorem 2.1: though the averaged quantities, ρ^{\pm} will be now decoupled through the low order p -dependent terms, weighted stability follows as before due to the antisymmetry of the leading term in (2.11a)-(2.11b). \square .

In our third corollary we note that the last two weighted L^2 -stability results apply equally well to higher order derivatives, which brings us to conclude with the following

Corollary 2.4. (Weighted W^α -Stability.) *Let $u_N(t) \equiv u_N(\cdot, t)$ denote the solution of the Fourier method*

$$(2.28) \quad \frac{\partial}{\partial t} u_N(x, t) = \frac{\partial}{\partial x} \psi_N [\sin(x) u_N(x, t)].$$

Then there exist positive definite matrices, $H_{\pm}^{(\alpha)}$, and a constant C_α , such that the following weighted W^α -stability estimate holds

$$(2.29) \quad \| \|u_N(t)\| \|_{W_H^\alpha} \leq C_\alpha(t) \| \|u_N(0)\| \|_{W_H^\alpha}$$

Here $\| \|u_N(t)\| \|_{W_H^\alpha}$ denotes the weighted W^α -norm

$$(2.30) \quad \| \|u_N(t)\| \|_{W_H^\alpha}^2 := \| \Lambda^\alpha \mathbb{R} \hat{u}(t) \|_{H_-^{(\alpha)}}^2 + \| \Lambda^\alpha \mathbb{I} \hat{u}(t) \|_{H_+^{(\alpha)}}^2.$$

Proof. Let $\tilde{\Lambda}$ denote the $2N \times 2N$ 'punctured' Λ matrix. If we set $T_\pm^{(\alpha)} := |\tilde{\Lambda}|^\alpha T_\pm |\tilde{\Lambda}|^{-\alpha}$, then we can rewrite (2.15)₋ as

$$T_-^{(\alpha)} |\tilde{\Lambda}|^\alpha \tilde{a}(t) = e^{-t/2} e^{\mathcal{F}^{(\alpha)} t/2} T_-^{(\alpha)} |\tilde{\Lambda}|^\alpha \tilde{a}(0),$$

and a similar relation holds for $\tilde{b}(t)$ in view of (2.15)₊. The essential point is that $e^{\mathcal{F}^{(\alpha)} t/2}$ is bounded and hence

$$\| \tilde{\Lambda}^\alpha \tilde{a}(t) \|_{H_-^{(\alpha)}} \leq e^{(C_\alpha - 1)t/2} \| \tilde{\Lambda}^\alpha \tilde{a}(0) \|_{H_-^{(\alpha)}}, \quad H_-^{(\alpha)} = T_-^{(\alpha)} T_-^{(\alpha)}.$$

We conclude by noting that $\tilde{\Lambda}^\alpha \tilde{a}(t) \equiv \Lambda^\alpha a(t)$ (since $\alpha > 0$), and (2.29) follows with $H = H_-^{(\alpha)} \oplus H_+^{(\alpha)}$. \square

The last results enable to put forward a complete weighted L^2 -stability theory. The following assertion contains the typical ingredients.

Assertion. The Fourier method

$$(2.31) \quad \frac{\partial}{\partial t} u_N(x, t) = \psi_N[\sin(x) \frac{\partial}{\partial x} u_N(x, t)],$$

satisfies the following weighted W^α -stability estimate

$$(2.32) \quad \| \|u_N(\cdot, t)\| \|_{W_H^\alpha} \leq C_\alpha(t) \| \|u_N(\cdot, 0)\| \|_{W_H^\alpha}.$$

Remark. The last assertion confirms the weighted stability of the Fourier method in its non-conservative transport form.

Sketch of the Proof. We rewrite (2.31) in the 'conservative form'

$$\frac{\partial}{\partial t} u_N(x, t) = \frac{\partial}{\partial x} \psi_N[\sin(x) u_N(x, t)] + \left[\psi_N \sin(x), \frac{\partial}{\partial x} \right] u_N(x, t),$$

where $[\psi_N \sin(x), \frac{\partial}{\partial x}] := \psi_N(\sin(x) \frac{\partial}{\partial x} \cdot) - \frac{\partial}{\partial x}(\psi_N \sin(x) \cdot)$ denotes the usual commutator between interpolation and differentiation. The weighted L^2 -stability stated in Theorem 2.1 tells us that this commutator is bounded in the corresponding weighted operator norm. Therefore, we may treat the right hand side of (2.31) as a low order term and weighted L^2 -stability ($\alpha = 0$) follows in view of Corollary 2.3. The case of general $\alpha > 0$ follows with the help of Corollary 2.4. \square

Table 1. Amplification of $\|u_N(t)\|$ at $t = 10$, subject to initial data $\hat{u}_\kappa(0) = i \sin(k\pi/N)$

$2N + 1$	65	129	257	513	1205
$\frac{\ u_N(t)\ }{\ u_N(0)\ }$	570	2003	5535	15028	39798

3. Algebraic stability and weak L^2 -instability

In this section we turn our attention to the behavior of the Fourier method (2.6) in terms of the L^2 -norm. Table 1 suggests that when measured with respect to the standard (weight-free) L^2 -norm, the Fourier approximation may grow linearly with the number of gridpoints N .

The main result of this section asserts that this is indeed the case.

Theorem 3.1. *There exist constants, $C_1(t)$ and $C_2(t)$, such that the following estimate holds*

$$(3.1) \quad C_1(t)N \leq \|e^{DQ_t}\| \leq C_2(t)N.$$

The right hand side of (3.1) tells us that the Fourier method may amplify the L^2 -size of its initial data by an amplification factor $\leq O(N)$ – that is, the Fourier method is *algebraically stable*. The left hand side of (3.1) asserts that this estimate is sharp in the sense that there exist initial data for which this $O(N)$ amplification is attained – that is, the Fourier method is *weakly L^2 -unstable*. We note that this estimate does not contradict the weighted L^2 -stability discussed in Sect. 2; in fact, as we shall see below, the weighted L^2 -stability reveals the mechanism for this algebraically weak L^2 -instability.

We turn to the *proof of the algebraic stability*. Let $u_N(t)$ denote the solution of the Fourier method (2.6) subject to arbitrary initial data, $u_N(0)$. We claim that we can bound the ratio $\|u_N(t)\|/\|u_N(0)\|$ in terms of the *condition number*, $\kappa(H)$, of the weighting matrix H , $\kappa(H) := \|H\| \cdot \|H^{-1}\|$. Indeed

$$\begin{aligned}
\|u_N(t)\| &= \|\mathbb{R}e\hat{u}(t) \oplus \mathbb{I}m\hat{u}(t)\| \leq \sqrt{\|H^{-1}\|} \cdot \|u_N(t)\|_H \\
&\leq C(t)\sqrt{\|H^{-1}\|} \cdot \|u_N(0)\|_H \\
(3.2) \quad &\leq C(t)\sqrt{\|H\| \cdot \|H^{-1}\|} \cdot \|\mathbb{R}e\hat{u}(0) \oplus \mathbb{I}m\hat{u}(0)\| \\
&= C(t)\sqrt{\kappa(H)} \cdot \|u_N(0)\|.
\end{aligned}$$

Here, the first and last equalities are Parseval's identities; the second and forth inequalities are straightforward by the definition of a weighted norm; and the third is a manifestation of the weighted L^2 -stability stated in Corollary 2.2.

The estimate (3.2) requires to upper-bound the condition number of the weighting matrix H . We recall that the weighting matrix H is the direct sum of the matrices H_\pm given in (2.21a)-(2.21b), whose L^2 -norms equal the squared L^2 -norms of the corresponding Jordan blocks, $\|H_\pm\| \equiv \|J_\pm\|^2$, $\|H_\pm^{-1}\| \equiv \|J_\pm^{-1}\|^2$. Inserting this into (3.2) we arrive at

$$(3.3) \quad \|e^{DQt}\| := \sup_{u_N(0) \neq 0} \frac{\|u_N(t)\|}{\|u_N(0)\|} \leq C(t)\kappa(J), \quad J := J_- \oplus J_+.$$

Thus it remains to upper bound the condition number of the Jordan blocks, J_{\pm} . For the sake of completeness we include a brief calculation of the latter. The inverse of J_{\pm} are upper-triangular Toeplitz matrices,

$$(3.4a) \quad (J_{\pm}^{-1})_{jk} = \begin{cases} (\mp 1)^{j-k} & k \geq j, \\ 0 & k < j, \end{cases}$$

for which we have,

$$(3.4b) \quad \|J_{\pm}^{-1}w\|^2 = \sum_{j=-N}^N \left| \sum_{k \geq j} (\mp 1)^{j-k} w_k \right|^2 \leq \sum_{j=-N}^N \sum_k |w_k|^2 \sum_{k \geq j} 1 \sim 2N^2 \|w\|^2.$$

This means that $\|J_{\pm}^{-1}\| \leq \sqrt{2}N$, and together with the straightforward upper-bound, $\|J_{\pm}\| \leq 2$, the right hand side of the inequality (3.1) now follows with $C_2(t) = 2\sqrt{2}C(t)$. \square

The above $O(N)$ -algebraic stability is essentially due to the $O(N)$ upper-bound on the size of the inverses of Jordan blocks stated in (3.4b). Can this upper-bound be improved? an affirmative answer to this question depends on the regularity of the data, as shown by the estimate

$$\|J_{\pm}^{-1}w\|^2 = \sum_{j=-N}^N \left| \sum_{k \geq j} (\mp 1)^{j-k} w_k \right|^2 \leq \sum_{j=-N}^N \sum_k |k|^{2\alpha} |w_k|^2 \sum_{k \geq j} |k|^{-2\alpha},$$

which yields an $O(N^{(1-\alpha)_+})$ bound for W^α -data,

$$\|J_{\pm}^{-1}w\| \leq C_{N,\alpha} N^{(1-\alpha)_+} \|w\|_{W^\alpha}, \quad \|w\|_{W^\alpha} := \left(\sum_k |k|^{2\alpha} |w_k|^2 \right)^{1/2}.$$

Noting that the rest of the arguments in the proof of algebraic stability are invariant with respect to the W^α -norm – in particular, the weighted W^α -stability stated in Corollary 2.4, we conclude the following extension of the right inequality in (3.1).

Corollary 3.2. (Weak W^α -stability estimate.) *There exist constants $C_{s,\alpha}$, $s, \alpha \geq 0$, such that the following estimate holds*

$$(3.5) \quad \|u_N(\cdot, t)\|_{W^s} \leq C_{N,s,\alpha} N^{(1-\alpha)_+} \|u_N(\cdot, 0)\|_{W^{s+\alpha}}.$$

$$\text{Here } C_{N,s,\alpha} = \begin{cases} \text{Const} \cdot \sqrt{\log N} & \alpha = \frac{1}{2}, 1, \\ \leq C_{s,\alpha} & \text{otherwise.} \end{cases}$$

Corollary 3.2 tells us how the smoothness of the initial data is related to the possible algebraic growth; actually, for W^α -initial data with $\alpha > 1$, there is no L^2 -growth. However, for arbitrary L^2 data ($s = \alpha = 0$) we remain with the $O(N)$ upper bound (3.4b), and this bound is indeed sharp for, say, $w_k \sim (-1)^k$. (In fact, the latter is reminiscent of the unstable oscillatory boundary wave we shall meet later in (3.20)).

These considerations lead us to the question whether the *linear* L^2 -growth upper-bound offered by the right hand side of (3.1) is sharp. To answer this question we return to take a closer look at the real and imaginary parts of our system (2.7).

We recall that according to (2.9a) the real part, $a_k(t) = \Re \hat{u}_k(t)$, satisfies,

$$\frac{d}{dt} a_k(t) = \frac{k}{2} [a_{k-1}(t) - a_{k+1}(t)], \quad -N \leq k \leq N.$$

Summing by parts against $a_k(t)$ we find

$$\frac{1}{2} \frac{d}{dt} \sum_{k=-N}^N a_k^2(t) = \frac{1}{2} \sum_{k=-N+1}^N a_k(t) a_{k-1}(t) - \frac{N}{2} [a_{-(N+1)}(t) a_{-N}(t) + a_{N+1}(t) a_N(t)].$$

The boundary conditions (2.9b), $a_{-(N+1)}(t) - a_{-N}(t) = a_{N+1}(t) - a_N(t) = 0$, imply that the second term on the right is positive; using Cauchy-Schwartz to upper bound the first term yields $\frac{d}{dt} \|a(t)\|^2 \leq \|a(t)\|^2$, which in turn implies that the real part of the system (2.7) is L^2 -stable

$$\|a(t)\| \leq e^{t/2} \|a(0)\|, \quad a(t) = \Re \hat{u}(t).$$

In contrast to the L^2 -bounded real part, it will be shown below that the imaginary part of our system experiences an L^2 linear growth, which is responsible for the algebraically weak L^2 -instability of the Fourier method.

The imaginary part of our system, $b(t) = \Im \hat{u}_k(t)$, satisfies the same recurrence relations as before

$$(3.6a) \quad \frac{d}{dt} b_k(t) = \frac{k}{2} [b_{k-1}(t) - b_{k+1}(t)], \quad -N \leq k \leq N,$$

the only difference lies in the augmenting boundary conditions which now read

$$(3.6b) \quad b_{-(N+1)}(t) = -b_{-N}(t), \quad b_{N+1}(t) = -b_N(t) = \mathbf{0}.$$

Trying to repeat our argument in the real case, we sum by parts against $b_k(t)$,

$$(3.7) \quad \frac{1}{2} \frac{d}{dt} \sum_{k=-N}^N b_k^2(t) = \frac{1}{2} \sum_{k=-N+1}^N b_k(t) b_{k-1}(t) - \frac{N}{2} [b_{-(N+1)}(t) b_{-N}(t) + b_{N+1}(t) b_N(t)],$$

but unlike the previous case, the judicious minus sign in the augmenting boundary conditions (3.6b) leads to the *lower* bound

$$(3.8) \quad \frac{d}{dt} \|b(t)\|^2 \geq -\|b(t)\|^2 + N[b_{-N}^2(t) + b_N^2(t)].$$

This lower bound indicates (but does not prove!) the possible L^2 -growth of the imaginary part. Figure 1 confirms that unlike the L^2 -bounded real part, the behavior of the imaginary part is indeed markedly different – it consists of binary oscillations which form a growing modulated wave as $|k| \uparrow N$. These *binary* oscillations suggest to consider $v_k(t) := (-1)^k b_k(t)$, in order to gain a better insight into the growth of the underlying modulated wave. Observe that (3.6a)-(3.6b) then recasts into the centered difference scheme

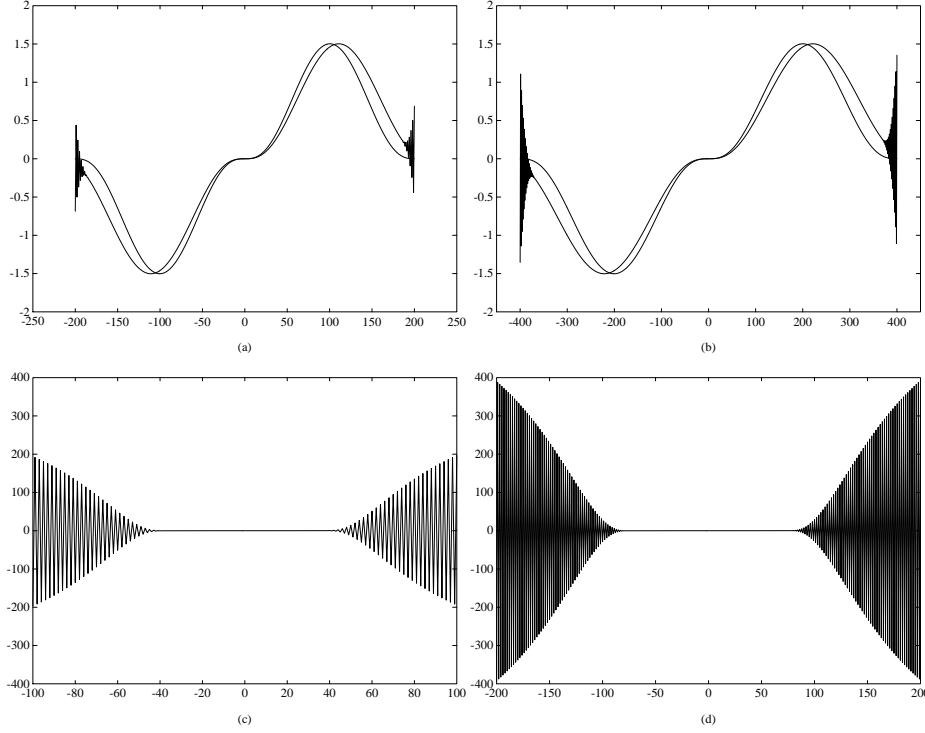


Fig. 1. a–d. Fourier solution of $u_t = (\sin(x)u)_x$, $\hat{u}_k(0) = \xi_k^2(\pi - \xi_k)^3/20$, $\xi_k = k\pi\Delta\xi$. Imaginary part of Fourier coefficients, $\Im\hat{u}_k(t)$, computed with $\Delta t = \frac{1}{5N}$ at **a** $t = 0$ and $t = 0.1$ with $N = 200$; **b** $t = 0$ and $t = 0.1$ with $N = 400$; **c** $t = 1$ with $N = 100$; **d** $t = 1$ with $N = 200$

$$(3.9a) \quad \frac{d}{dt} v_k(t) = \xi_k \frac{v_{k+1}(t) - v_{k-1}(t)}{2\Delta\xi}, \quad \xi_k := k\Delta\xi, \quad 0 \leq k \leq N, \quad \Delta\xi := \frac{1}{N + \frac{1}{2}},$$

which is augmented with first order homogeneous extrapolation at the 'right' boundary

$$(3.9b) \quad v_{N+1}(t) - v_N(t) = 0.$$

We note in passing that {i} The $b_k(t)$'s, and hence the $v_k(t)$'s, are symmetric – in this case they have an odd extension for $-N \leq k \leq 0$; {ii} No additional boundary condition is required at the left characteristic boundary $\xi_0 = 0$; and finally, {iii} Though (3.9a)-(3.9b) are independent of the frequency spacing — in fact any $\Delta\xi = O(1/N)$ will do, yet the choice of $\Delta\xi = (N + \frac{1}{2})^{-1}$ will greatly simplify the formulae obtained below. These simplifications will be advantageous throughout the rest of this section.

Clearly, the centered difference scheme (3.9a) could be viewed as a consistent approximation to the linear wave equation

$$\frac{\partial}{\partial t} v(\xi, t) = \xi \frac{\partial}{\partial \xi} v(\xi, t), \quad 0 \leq \xi \leq 1.$$

The essential point is that $\xi = 1$ is an *inflow* boundary in this case, and that the boundary condition (3.9b) is *inflow-dependent* in the sense that it is consistent with the

interior inflow problem. Such inflow-dependent boundary condition renders the related constant coefficient approximation *unstable*, that is, the mixed initial-boundary value approximation (3.9a)-(3.9b) with 'frozen' coefficients, fails to satisfy the resolvent-type stability of Gustafsson, Kreiss and Sundström [GKS], consult [KL, Os, Ta1, Tr]. In fact, the instability induced by using such first-order extrapolation (3.9b) in an *inflow* boundary leads to an L^2 -growth of order $\geq O(\sqrt{N})$, consult [Ta1, Sect. 3].

To show that there is an $O(N)$ -growth in this case requires a more precise study along these lines, which brings us to the *proof of the weak L^2 -instability*. We decompose the imaginary components, $b_k(t)$, as the sum of two contributions – a stable part, $s_k(t)$, associated with the evolution of the initial data; and an unstable part, $\omega_k(t)$, which describes the unstable binary oscillations propagating from the boundaries into the interior domain,

$$b_k(t) \equiv s_k(t) + \omega_k(t).$$

Here, $s(t) := (s_1(t), \dots, s_N(t))$ is governed by an *outflow* centered difference scheme which is complemented by *stable* boundary extrapolation,

$$(3.10) \quad \begin{cases} \frac{d}{dt} s_k(t) + \xi_k \frac{s_{k+1}(t) - s_{k-1}(t)}{2\Delta\xi} = 0, & 0 \leq k \leq N, & \Delta\xi := \frac{1}{N + \frac{1}{2}} \\ s_k(0) = b_k(0), \\ s_{N+1}(t) = s_N(t). \end{cases}$$

As before, we exploit symmetry to confine our attention to the 'right half' of the problem, $0 \leq k \leq N$.

A straightforward L^2 -energy estimate confirms that this part of the imaginary components is L^2 -stable, $\|s(t)\| \leq e^{-t} \|b(0)\|$. In fact, the scheme (3.10) retains high-order stability in the sense that

$$(3.11) \quad \|s(t)\|_{W^\alpha} = \left(\sum_{k=0}^N |k|^{2\alpha} |s_k(t)|^2 \right)^{1/2} \leq \text{Const}_{\alpha,t} \cdot \|b(0)\|_{W^\alpha}, \quad \forall \alpha \geq 0.$$

We close our discussion on the so called "s"-part by noting that (3.10) is a second-order accurate approximation to the initial-value problem

$$(3.12) \quad \begin{cases} \frac{\partial}{\partial t} s(\xi, t) + \xi \frac{\partial}{\partial \xi} s(\xi, t) = 0, & \xi \geq 0, \\ s(\xi, 0) = b(\xi), & b(\xi) := \frac{-1}{2N+1} \sum_{\nu=0}^{2N} u_N(x_\nu, 0) \sin(\pi\nu\xi); \end{cases}$$

Observe that the initial condition $b(\xi)$ is nothing but a trigonometric interpolant in the frequency ' ξ -space', which coincides with the initial value of the imaginary components, $b(\xi_k) = \mathbb{I}m \hat{u}_k(0) \equiv b_k(0)$. Using the explicit solution of this initial value problem, we end up with a second order convergence statement which reads³

$$(3.13) \quad s_k(t) = b(\xi_k e^{-t}) + O(\Delta\xi)^2, \quad t \geq 0.$$

We now turn our attention to the unstable oscillatory part, $\omega_k(t) = (-1)^{N-k} v_k(t)$. It is governed by an *inflow* centered difference scheme,

³ The last equality should be interpreted of course in the W^α -sense, with α limited by the initial W^α -smoothness of $b_k(0)$.

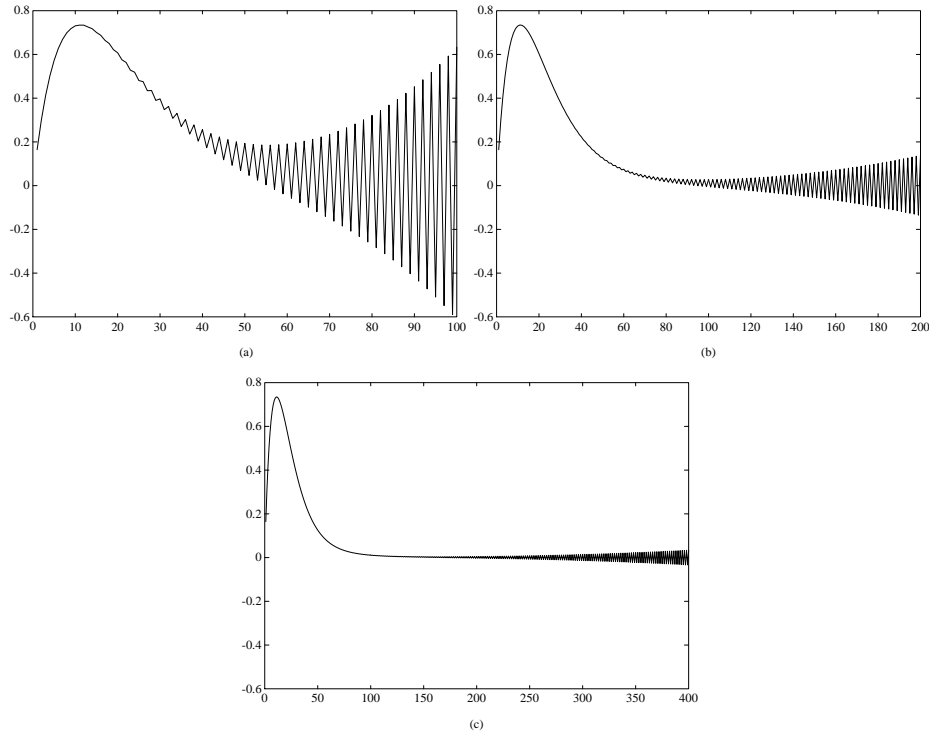


Fig. 2. a–c. Fourier solution of $u_t = (\sin(x)u)_x$, $\hat{u}_k(0) \sim \frac{i}{k^3}$. Imaginary part of Fourier coefficients, $\Im \hat{u}_k(t)$, computed at $t = 3$ with $\Delta t = \frac{1}{10N}$ and **a** with $N = 100$; **b** with $N = 200$; **c** with $N = 800$

$$(3.14a) \quad \begin{cases} \frac{d}{dt} v_k(t) &= \xi_k \frac{v_{k+1}(t) - v_{k-1}(t)}{2\Delta\xi}, & 0 \leq k \leq N, \\ v_k(0) &\equiv 0, \end{cases}$$

which is coupled to the previous stable "s"-part (3.10), through the boundary condition

$$(3.14b) \quad v_{N+1}(t) - v_N(t) = s_{N+1}(t) + s_N(t).$$

The boundary condition (3.14b) is the first-order accurate extrapolation we met earlier in (3.9b) – but this time, with the additional inhomogeneous boundary data. And as before, a key ingredient in the L^2 -instability is the fact that such boundary treatment is inflow-dependent.

Specifically, we claim: *the inflow-dependent extrapolation on the left of (3.14b) reflects the boundary values on the right of (3.14b), which are 'inflowed' into the interior domain with an amplitude amplified by a factor of order $O(N)$.*

To prove this claim we proceed as follows. Forward differencing of (3.14a) implies that $r_{k+\frac{1}{2}}(t) := v_{k+1}(t) - v_k(t)$ satisfy the stable difference scheme

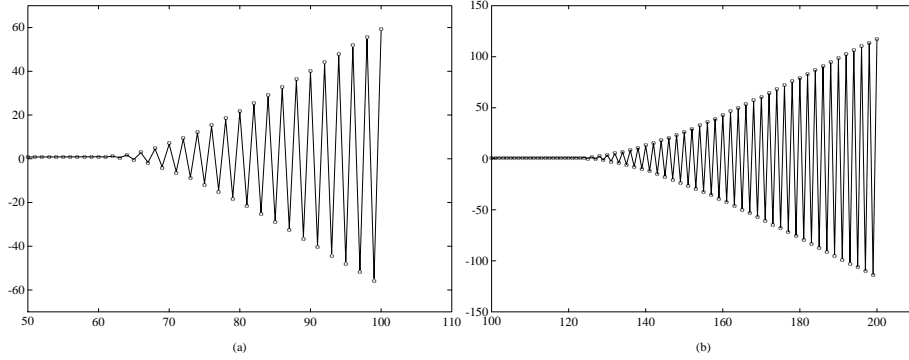


Fig. 3. a,b. Fourier solution of $u_t = (\sin(x)u)_x$, $\hat{u}_k(0) = i \sin(\xi_k)$, $\xi_k = k\pi\Delta\xi$. Imaginary part of Fourier coefficients, $\Im\hat{u}_k(t)$, (---) computed at $t = 0.5$ vs. $s_k(t) + \omega_k(t)$, (ooo), **a** with $N = 100$; **b** with $N = 200$

$$(3.15) \quad \begin{cases} \frac{d}{dt} r_{k+\frac{1}{2}}(t) = \frac{\xi_{k+\frac{3}{2}} r_{k+\frac{3}{2}}(t) - \xi_{k-\frac{1}{2}} r_{k-\frac{1}{2}}(t)}{2\Delta\xi} - \frac{r_{k+\frac{3}{2}}(t) - 2r_{k+\frac{1}{2}}(t) + r_{k-\frac{1}{2}}(t)}{4}, & k \leq N-1, \\ r_{k+\frac{1}{2}}(0) \equiv 0, \\ r_{N+\frac{1}{2}}(t) = s_{N+1}(t) + s_N(t) \equiv 2s_N(t). \end{cases}$$

Clearly, this difference scheme is consistent with, and hence convergent to the solution of the initial-boundary value problem

$$(3.16) \quad \begin{cases} \frac{\partial}{\partial t} r(\xi, t) = \frac{\partial}{\partial \xi} (\xi r(\xi, t)), & 0 \leq \xi \leq 1, \\ r(\xi, 0) \equiv 0 \\ r(1, t) = 2s_N(t). \end{cases}$$

Observe that $r(\xi, t)$ describes a boundary wave which is prescribed on the $\xi_{N+\frac{1}{2}} = 1$ boundary of the computed spectrum, $r(1, t) = 2s_N(t)$, and propagates into the interior domain of lower frequencies $\xi < 1$,

$$(3.17) \quad r(\xi, t) = \begin{cases} \frac{2}{\xi} s_N(t + \ln \xi), & t + \ln \xi \geq 0, \\ 0, & t + \ln \xi \leq 0. \end{cases}$$

We conclude that the forward differences, $r_{k+\frac{1}{2}}(t) = v_{k+1}(t) - v_k(t)$, form a second-order accurate approximation of this boundary wave,

$$r_{k+\frac{1}{2}}(t) = r(\xi_{k+\frac{1}{2}}, t) + O(\Delta\xi)^2, \quad \xi_{k+\frac{1}{2}} = (k + \frac{1}{2})\Delta\xi.$$

Returning to the original variables, $\omega_k(t) \equiv (-1)^k \sum_{j=0}^{k-1} r_{j+\frac{1}{2}}(t)$, the latter equality reads

$$\begin{aligned}
(3.18) \quad \omega_k(t) &= (-1)^k \sum_{j=0}^{k-1} r(\xi_{j+\frac{1}{2}}, t) + O(k(\Delta\xi)^2) \\
&= \frac{(-1)^k}{\Delta\xi} R(\xi_k, t) + O(\Delta\xi), \quad R(\xi_k, t) := \int_{e^{-t}}^{\xi_k} r(\xi, t) d\xi,
\end{aligned}$$

which confirms our above claim regarding the amplification of a boundary wave by a factor of $O(1/\Delta\xi \sim N)$.

The a priori estimates (3.11) and (3.18) provide us with precise information on the behavior of the imaginary components, $b(t) = s(t) + \omega(t)$: their initial value at $t = 0$ propagate by the stable "s"-part and reaches the boundary of the computed spectrum at $\xi_{N+\frac{1}{2}} = 1$ with the approximate boundary values of (3.13), $s_N(t) = b(e^{-t}) + O(\Delta\xi)$; the latter propagate into the interior spectrum as a boundary wave of the form (3.17), $r(\xi, t) = \frac{2}{\xi} b(\frac{1}{\xi e^t})$, whose primitive in (3.18) describes the unstable oscillatory "ω"-part of the solution. Added all together we end up with

$$(3.19) \quad b_k(t) = b(\xi_k e^{-t}) + \left\{ \begin{array}{l} \frac{2(-1)^k}{\Delta\xi} \int_{\xi \geq e^{-t}/\xi_k}^1 b(\xi) \frac{d\xi}{\xi}, \quad e^{-t} \leq \xi_k \leq 1 \\ 0, \quad 0 \leq \xi_k \leq e^{-t} \end{array} \right\} + O(\Delta\xi).$$

Thus, the unstable "ω"-part contributes a wave which is modulated by binary oscillations; the amplitude of these oscillations start with $O(1/\Delta\xi \sim N)$ amplification near the boundary of the computed spectrum, $\xi_N \sim 1$, and decreases as they propagate into the interior domain of lower frequencies. Moreover, for any fixed $t > 0$, only those modes with wavenumber k such that $e^{-t} < |k|/N \leq 1$, are affected by the unstable "ω" part. Put differently, we state this as

Corollary 3.3. *For any fixed $t > 0$, the Fourier method (2.6) experiences a weak instability which affects only a fixed fraction of the computed spectrum. Yet, the size of this fixed fraction, $1 - e^{-t}$, approaches unity exponentially fast in time.*

There are two different cases to be considered, depending on the smoothness of the initial data.

1. *Smooth initial data.* If the initial data $u_N(x, 0)$ are sufficiently smooth, then $b_k(0) = \text{Im} \hat{u}_k(0)$ are rapidly decaying as $|k| \uparrow N$, and hence – by the W^α -stability of the "s"-part in (3.11), this rapid decay is retained later in time for $s_k(t)$, $t > 0$. This implies that the discrete boundary wave – governed by the stable scheme (3.15), is negligibly small, $r_{k+\frac{1}{2}}(t) \approx 0$, because its boundary values are, $2s_N(t) \approx 0$. We conclude that in the smooth case, $\|b(t)\| \sim \|b(0)\| + O(1)$ remains of the same size as its initial data, $\|b(0)\|$.

Figure 2 demonstrates this result for a prototype case of smooth initial data in Besov $B_\infty^3(L^\infty)$ – in this case, initial data with cubically decaying imaginary components, $b_k(0) \sim |k|^{-3}$. As told by (3.19), the temporal evolution of these components should include an amplified oscillatory boundary wave, $\omega_k(t) \sim (-1)^k k^3 N^{-5}$, consult Remark 3 below. This $O(N)$ amplification is confirmed by the quadratic decay of the boundary amplitudes, $\omega_N(t)$. Note that despite this amplification, the boundary wave and hence the whole Fourier solution remain L^2 bounded in this smooth case.

2. *Nonsmooth initial data.* We consider initial data $u_N(x, 0)$ with very low degree of smoothness beyond their mere L^2 -integrability, e.g., for $b(\xi) = N^{-1/2}(1 - \xi)$, the corresponding components of $\mathbb{I}m \hat{u}_k(0) = N^{-1/2}(1 - \frac{k}{N})$, are square summable but slowly decaying as $|k| \uparrow N$. Since $b(0)$ serves as initial data for the stable "s"-part in (3.10), the components of $s_k(t)$ will remain square summable for $t > 0$, but will remain slowly decaying as $|k| \uparrow N$. In particular, this means that $s_N(t) = O(N^{-1/2})$ can be used to create the $O(N^{-1/2})$ boundary wave $r(\xi, t)$ dictated by (3.16). According to (3.18), the amplified primitive of this boundary wave, $(-1)^k R(\xi_k, t)/\Delta\xi \sim N^{1/2}$, will serve as the leading order term of the unstable part. We conclude that the imaginary part $\|b(t)\|$ will be amplified by a factor of $O(N)$ relative to the size of its nonsmooth initial data $\|b(0)\|$, which confirms the left hand side of the inequality (3.1).

Figure 3 demonstrates this result for a prototype case of nonsmooth initial data with imaginary components given by, $b_k(0) = \sin(\xi_k)$, that is, initial data represented by a strongly peaked dipole at $x_{\pm 1}$, $u_N(x_\nu, 0) = (2N + 1)\delta_{|\nu|, 1}$. According to (3.19), the evolution of these components in time yields

$$(3.20) \quad b_k(t) \sim \sin(\xi_k e^{-t}) + Const_k \frac{(-1)^k}{\Delta\xi} \left(1 - \frac{1}{\xi_k e^{-t}} \right)_+ + O(\Delta\xi).$$

In this case the $O(N)$ oscillatory boundary wave, $\frac{(-1)^k}{\Delta\xi} \left(1 - \frac{1}{\xi_k e^{-t}} \right)_+$, is added to the $O(1)$ -initial conditions, $\sin(\xi_k)$, which is responsible for the L^2 -growth of order $O(N)$. This linear L^2 -growth is even more apparent with the 'rough' initial data we met earlier in Figure 1.

Remarks.

1. *Smoothing.* The last Theorem confirms the L^2 -instability indicated previously by the lower bound (3.8),

$$\frac{d}{dt} \|b(t)\|^2 \geq -\|b(t)\|^2 + N [b_{-N}^2 + b_N^2].$$

By the same token, summation by parts of the imaginary part (3.7), leads to the *upper* bound

$$\frac{d}{dt} \|b(t)\|^2 \leq \|b(t)\|^2 + N [b_{-N}^2 + b_N^2],$$

which shows that *had* the boundary values of the computed spectrum – which in this case consist of the last single mode $b_{\pm N}(t)$, were to remain relatively small, then the imaginary part – and consequently the whole Fourier approximation would have been L^2 -stable. For example, the rather weak *a priori* bound will suffice

$$(3.21) \quad |b_{\pm N}(t)| \leq \frac{C}{\sqrt{N}} \|b(0)\| \implies \|b(t)\| \leq e^{(1/2+C^2)t} \|b(0)\|.$$

What we have shown (in the second part of Theorem 3.1) is that such an a priori bound does not hold for general nonsmooth L^2 -initial data, where according to (3.19), $b_N(t) \sim O(N)\|b(t)\|$.

We recall that there are various procedures which enforce stability of the Fourier method, without sacrificing its high order accuracy. One possibility is to use the skew-symmetric formulation of our problem [KO1, GO]. Another possibility is based on

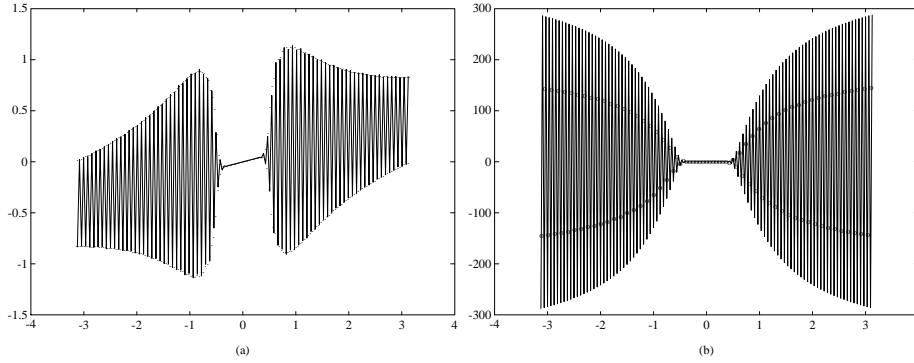


Fig. 4. a,b. Fourier solution of $u_t = (\sin(x)u)_x$, $\hat{u}(\xi, 0) = \sin(\xi)$. Imaginary part of Fourier coefficients, $\Im \hat{u}_k(t)$ vs. $k\pi\Delta\xi$, computed at $t = 2$ **a** with de-aliasing ($N = 80$ and $N = 160$); **b** without de-aliasing ($N = 50$ and $N = 100$)

the observation that the current instability is due to the inflow-dependent boundary conditions (3.9b) – or equivalently (3.6b), and the origin of the latter could be traced back to the aliasing relations (2.1b). We can therefore de-alias and hence by (3.21) stabilize the Fourier method by setting $b_{\pm N}(t) \equiv 0$, or more generally, $\hat{u}_{\pm N}(t) \equiv 0$. De-aliasing could be viewed as a robust form of high-frequency smoothing; in this context we mention the various high-frequency smoothing procedures which could be carried out either in the Fourier space as in Kreiss and Oliger [KO2] or Majda McDonough and Osher [MMO], in the physical space as in Abarbanel Gottlieb and Tadmor [GTa],[AGT], or could be realized as high-order spectral viscosity as in Tadmor [Ta3]. Figure 4a shows how the de-aliasing procedure stabilize the Fourier method which otherwise experiences the unstable linear growth in Fig. 4b. With (3.21) in mind, we may interpret these procedures as a mean to provide the missing a priori decaying bounds on the highest mode(s) of the computed spectrum, which in turn guarantee the stability of the whole Fourier approximation.

2. *Smoothing cont'd – even number of gridpoints.* The situation described in the previous remark is a special case of the following assertion [Ta2, p.545]: *Assume that $q(x)$ consists of a finite number, say m modes. Then the corresponding Fourier approximation (2.3) is L^2 -stable, provided the last m modes were smoothed so that the following a priori bound holds*

$$\sum_{|k|>N-m}^N |\hat{u}_k(t)|^2 \leq \frac{1}{N} \|b(0)\|^2.$$

It should be noted that our present discussion of $q(x)$ with $m = 1$ modes is a prototype case for the behavior of the Fourier method, as long as the corresponding Fourier approximation is based on an *odd* number of $2N + 1$ gridpoints. Otherwise – the case of an even number of gridpoints is L^2 -stable, as shown by Gottlieb, Orszag and Turkel [GOT]. The unique feature of this L^2 -stability is due to the fact that Fourier differentiation matrix in this case, $D_{jk} = \frac{(-1)^{j-k}}{2} \cot(\frac{x_j - x_k}{2})(1 - \delta_{jk})$ – being *even* order antisymmetric matrix, must have zero as a *double* eigenvalue, which in turn inflicts a 'built-in' smoothing of the last mode in this case, [Ta2, p.545], namely,

$$(3.22) \quad b_{\pm N}(t) \equiv 0.$$

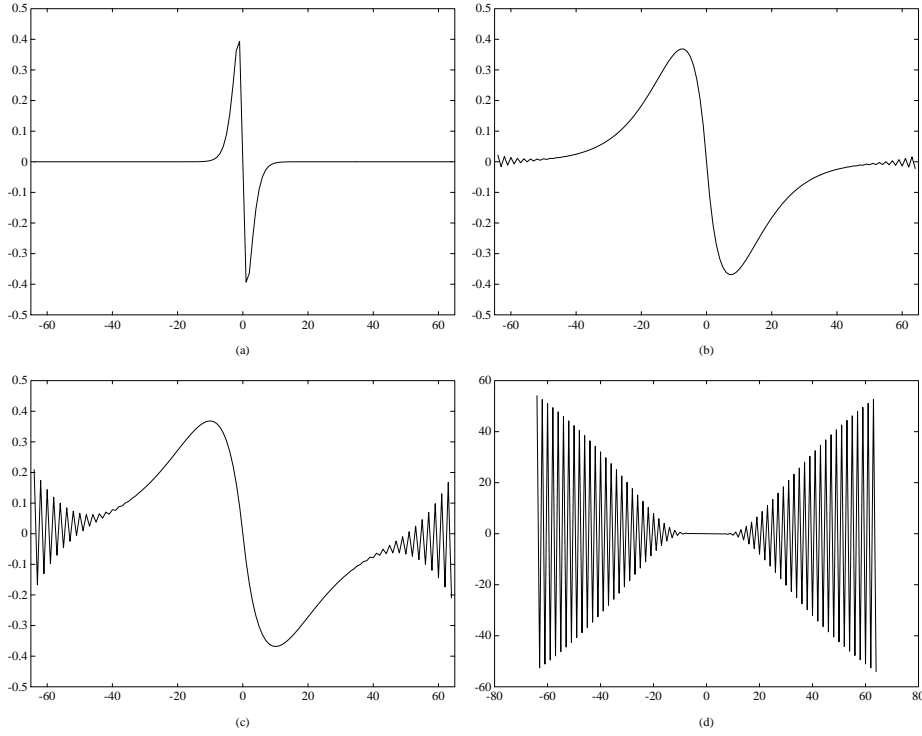


Fig. 5. a–d. Fourier solution of $u_t = (\sin(x)u)_x$, $u(x, 0) = \sin(x)$. Imaginary part of Fourier coefficients, $\Im \hat{u}_k(t)$, computed with $N = 64$ modes at **a** $t = 1.0$; **b** $t = 2.7$; **c** $t = 3.0$; **d** $t = 5.0$

Table 2 confirms the usual linear weak L^2 -instability already for a 2-wave coefficient.

3. W^α -initial data. Consider the case of sufficiently smooth initial data so that the imaginary components decay of order α ,

$$b_k(0) \sim |k|^{-\alpha}, \quad \alpha > \frac{1}{2}.$$

In this case, we may approximate the corresponding initial interpolant $b(\xi) \sim (\Delta\xi/\xi)^\alpha$, and (3.19) tells us the Fourier approximation takes the approximate form

$$\begin{aligned} b_k(t) &= \frac{e^{\alpha t}}{k^\alpha} + \frac{2(-1)^k}{\Delta\xi} \int_{\xi \geq e^{-t}/\xi_k}^1 \frac{(\Delta\xi)^\alpha}{\xi^{\alpha+1}} d\xi + O(\Delta\xi) \\ &\sim \frac{e^{\alpha t}}{k^\alpha} + \frac{(-1)^k}{N^{\alpha-1}} \left[\left(\frac{ke^t}{N} \right)_+^\alpha - 1 \right] + O(\Delta\xi). \end{aligned}$$

Observe that $\|b(t)\| \sim C_\alpha N^{\frac{3}{2}-\alpha}$, (with $C_\alpha \sim (e^{2\alpha t} - 1)/(2\alpha + 1)$), where as $\|b(0)\|_{W^\alpha} \sim \sqrt{N}$. This lower bound is found to be in complete agreement with the W^α -stability statement of Corollary 3.2 (apart from the $\log N$ factor for $\alpha = 1$) – an enjoyable sharpness.

Table 2. Amplification of $\|u_N(t)\|$ at $t = 5$ with even number of gridpoints. Here, $\frac{\partial}{\partial t} u_N(x, t) = \frac{\partial}{\partial x} \psi_N(\sin(2x)u_N(x, t))$, $u_N(x, 0) = \sin(x)$

$2N$	64	128	256	512
$\frac{\ u_N(t)\ }{\ u_N(0)\ }$	366	712	1906	5152

4. Stability resolution and convergence

In the previous sections we analyzed the stability of Fourier method in terms of two main ingredients: weighted L^2 -stability on the one hand, and high frequencies instability on the other hand. In this section we show how *both* of these ingredients contribute to the actual performance of the Fourier method.

We first address the issue of *resolution*. We left Sect. 3 with the impression that the weak L^2 -instability is a rather 'rare occurrence', as it is excited only in the presence of nonsmooth initial data. But in fact, the mechanism of this weak L^2 -instability will be excited whenever the Fourier method lacks enough resolution.

In this context let us first note that the solution of the underlying hyperbolic problem may develop large spatial gradients due to the almost impinging characteristics along the zeroes of the increasing part of $q(x)$. Consequently, the Fourier method might not have enough modes to resolve these large gradients as they grow in time. This tells us that independent whether the initial data are smooth or not, the computed approximation will then 'see' the underlying solution as a nonsmooth one, and this lack of resolution will be recorded by a slower decay of the computed Fourier modes. The latter will experience the high-frequency instability discussed earlier and this in turn will lead to the linear L^2 -growth. Our prototype example of $q(x) = \sin(x)$ is case in point: according to Corollary 3.3, one needs here at least $N \gg e^t$ modes in order to resolve the solution, for otherwise, (3.19) shows that spurious $O(N)$ oscillations will contaminate the whole computed spectrum.

We conclude that the lack of resolution manifests itself as a weak L^2 -instability. This phenomenon is demonstrated in Figs. 5–9, describing the Fourier method (2.6) subject to (the perfectly smooth ...) initial condition, $u(x, 0) = \sin(x)$. Figure 5 shows how the Fourier method with fixed number of $N = 64$ modes propagates information regarding the steepening of the Fourier solution in physical space, from low modes to the high ones. And, as this information is being transferred to the high modes, their $O(N)$ amplification become more noticeable as time progresses in Figs. 5c–d. Consequently, though $N = 64$ modes are sufficient to resolve the exact solution at $t \leq 2.7$, Fig. 6c–d shows that at later time, $t = 3$ and in particular $t = 5$, the under resolved Fourier solution with 64-modes will be completely dominated by the spurious centered spike. This loss of resolution requires more modes as time progresses. Figure 7 shows how the Fourier method is able to resolve the exact solution at $t = 3.5$, once 'sufficiently many' modes, $N \gg e^{3.5}$ are used, in agreement with Corollary 3.3. According to Figs. 8 and 9, $N = 512 \gg e^4$ modes are required to correctly resolve the two strong boundary dipoles at $t = 4$, yet at $t = 8$ the Fourier solution will be completely dominated by the spurious centered spike.

Assuming that the Fourier method contains sufficiently many modes dictated by the requirement of resolution, we now turn to the second issue of this section concern-

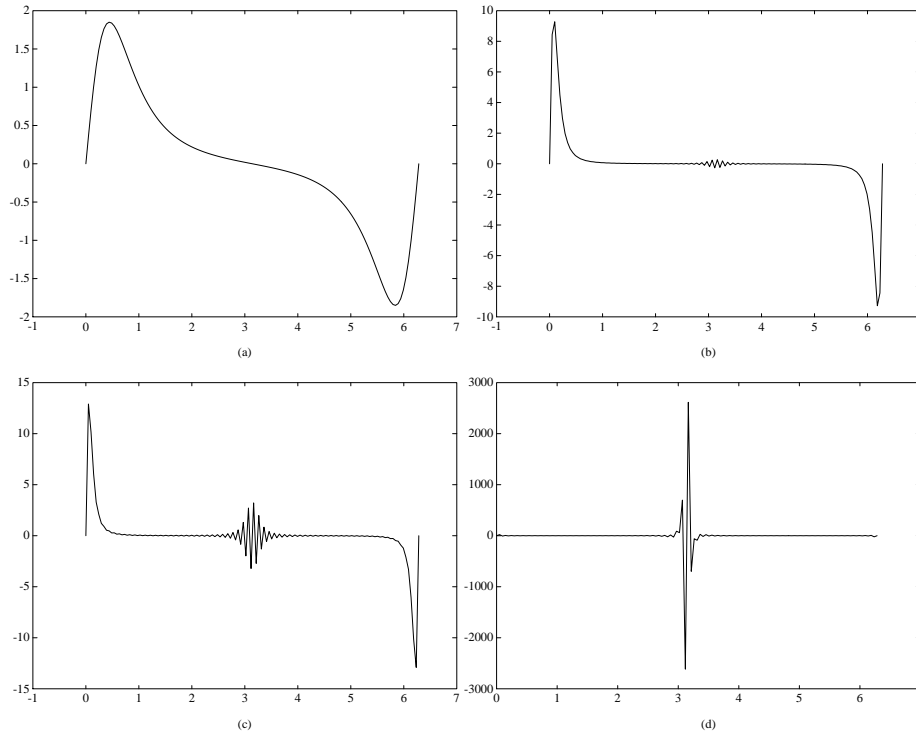


Fig. 6. a–d. Fourier solution of $u_t = (\sin(x)u)_x$, $u(x,0) = \sin(x)$. Computed solution, $u_N(\cdot, t)$, with $N = 64$ modes at **a** $t = 1.0$; **b** $t = 2.7$; **c** $t = 3.0$; **d** $t = 5.0$

ing the *convergence of the Fourier method*. Here, a straightforward approach would be to apply the weak L^2 -stability estimate (3.5) to the error equation,

$$(4.1) \quad \frac{\partial}{\partial t} e_N(x, t) = \frac{\partial}{\partial x} (\sin(x)e_N(x, t)) + F_N(x, t), \quad e_N(x, t) := u_N(x, t) - \psi_N u(x, t),$$

where $F_N(x, t)$ denotes the spectrally small truncation error. This L^2 -style approach is limited due to two related reasons:

- For practical purposes one is interested of course in higher, W^s -convergence estimates. To this end one notes that spatial derivatives of the error, $\frac{\partial^s}{\partial x^s} e_N(x, t)$, satisfy the same error equation as in (4.1), modulo the additional low order terms. However, the weak L^2 -stability estimate is *not* invariant in the presence of such low order terms;
- Moreover, the ‘low order terms’ mentioned above are in fact not small – they involve the L^2 -unbounded commutator, $[\psi_N \sin(x), \frac{\partial}{\partial x}]$, and its higher order variants⁴. Indeed, this commutator equals up to unitary equivalence to $\Re e DQ$, and the latter cannot be L^2 -bounded in view of the weak L^2 -instability stated in Theorem 3.1. In fact, it was noticed already in [KO1, p.204] that the L^2 -size of this commutator is of order $O(N)$.

⁴ Though this commutator is bounded in the *weighted* L^2 -norm – a fact that was already used in the closing remark of Sect. 2.

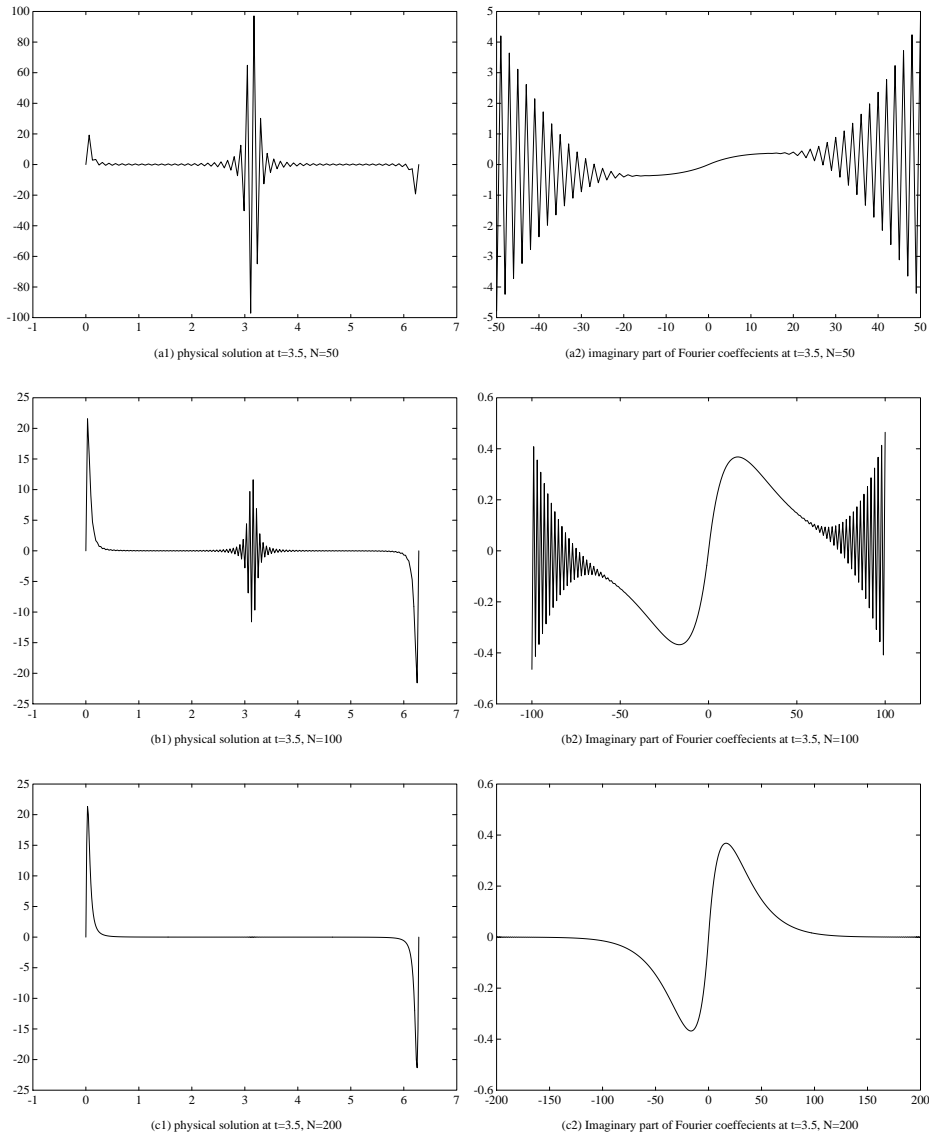


Fig. 7. a-c. Fourier solution of $u_t = (\sin(x)u)_x$, $u(x, 0) = \sin(x)$. Approximate solution, $u_N(\cdot, t)$ and imaginary part of its Fourier coefficients, $\Im \hat{u}_k(t)$ at $t = 3.5$ **a** with $N = 50$; **b** with $N = 100$; **c** with $N = 200$

What saves the day is the *weighted* L^2 -stability of the Fourier method. This brings us to the following.

Theorem 4.1. (Convergence rate estimate.) *Let $u_N(x, t)$ denotes the N -degree Fourier approximation of the corresponding exact solution $u(x, t)$. Then the following error estimate holds*

$$(4.2) \quad \|u_N(\cdot, t) - u(\cdot, t)\|_{W^s} \leq \text{Const}_{s,\alpha} N^{2-\alpha} \|u(\cdot, 0)\|_{W^{s+\alpha}}, \quad \forall s + \alpha > \frac{1}{2}.$$

Remark. The requirement from the initial data to have at least $W^{1/2}$ -regularity is clearly necessary in order to make sense of its *pointwise* interpolant.

Proof. We consider the error equation

$$(4.3a) \quad \frac{\partial}{\partial t}(u_N(x, t) - u(x, t)) = \frac{\partial}{\partial x} [\sin(x)(u_N(x, t) - u(x, t))] + F^{(N)}(x, t),$$

with the local error, $F^{(N)}(x, t)$, given by

$$(4.3b) \quad F^{(N)}(x, t) := \frac{\partial}{\partial x} [(\psi_N - I) \sin(x) u_N(x, t)].$$

Next we invoke two classical a priori estimates: a W^s -stability estimate on the inhomogeneous hyperbolic equation (4.3a) which yields

$$(4.4) \quad \|u_N(\cdot, t) - u(\cdot, t)\|_{W^s} \leq e^{C_s t} \cdot \left\{ \|u_N(\cdot, 0) - u(\cdot, 0)\|_{W^s} + \sup_{0 \leq \tau \leq t} \|F^{(N)}(\cdot, \tau)\|_{W^s} \right\};$$

and a canonical error estimate for Fourier interpolants, e.g., [Ta4, 1.2.17], stating that

$$(4.5) \quad \|(\psi_N - I)w(x)\|_{W^s} \leq C_{s,r} N^{s-r} \|w(x)\|_{W^r}, \quad \forall r \geq \max(s, \frac{1}{2}).$$

Now, application of (4.5) to $F^{(N)}(\cdot, \tau)$ yields

$$\|F^{(N)}(\cdot, \tau)\|_{W^s} \leq \|(\psi_N - I) \sin(\cdot) u_N(\cdot, \tau)\|_{W^{s+1}} \leq \text{Const}_{s,\alpha} N^{-\alpha} \|u_N(\cdot, \tau)\|_{W^{s+\alpha+1}}.$$

The weak stability statement in Corollary 3.2 allows us to upper bound the right hand side of the last inequality in terms of the initial data,

$$\begin{aligned} \|F^{(N)}(\cdot, \tau)\|_{W^s} &\leq \text{Const}_{s,\alpha} N^{1-\alpha} \|u_N(\cdot, \tau)\|_{W^{s+\alpha}} \\ &\leq \text{Const}_{s,\alpha} N^{2-\alpha} \|u_N(\cdot, 0)\|_{W^{s+\alpha}}. \end{aligned}$$

Also, application of (4.5) to $u_N(\cdot, 0) - u(\cdot, 0) = (\psi_N - I)u(\cdot, 0)$ yields

$$\|u_N(\cdot, 0) - u(\cdot, 0)\|_{W^s} \leq \text{Const}_{s,\alpha} N^{-\alpha} \|u_N(\cdot, 0)\|_{W^{s+\alpha}}, \quad s + \alpha \geq \frac{1}{2}.$$

The inequality (4.4) complemented with the last two upper-bounds yield the desired result (4.2). \square

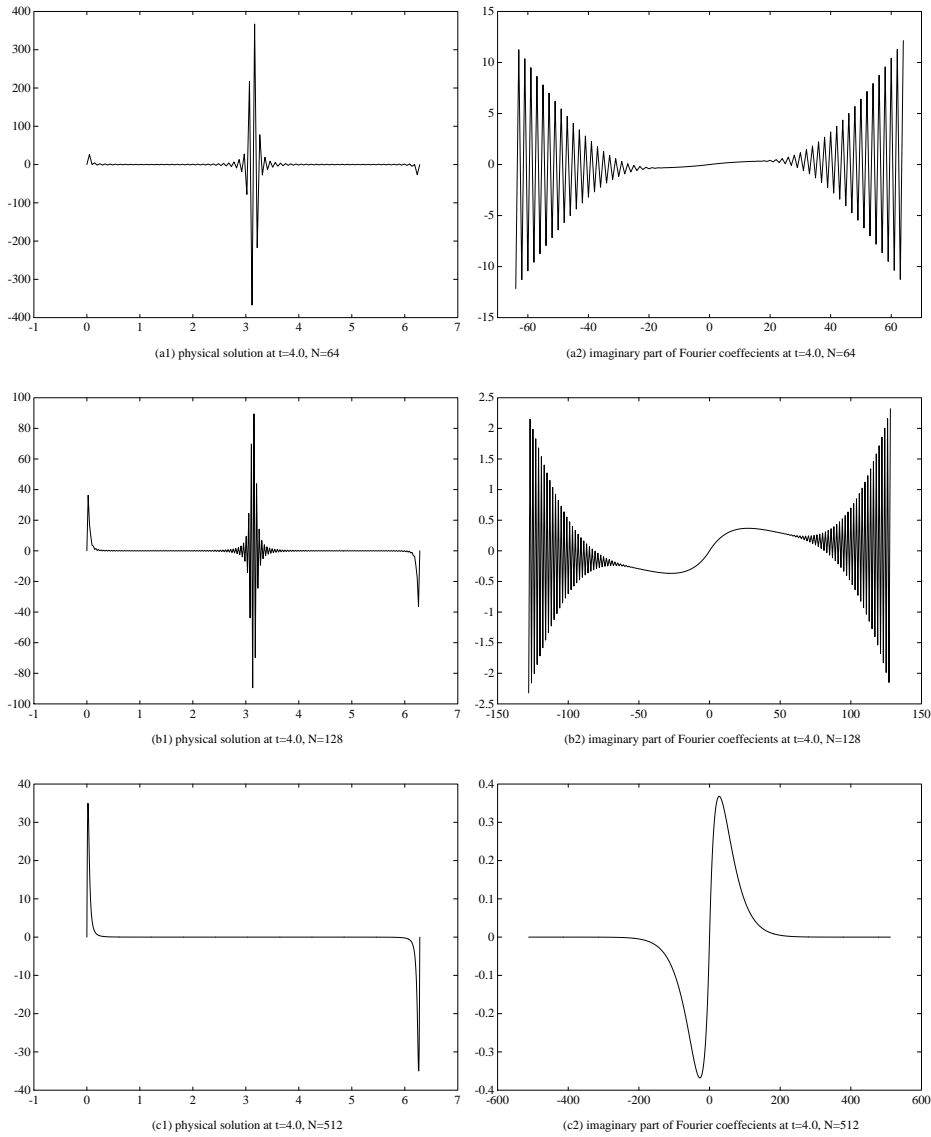


Fig. 8. a–c. Fourier solution of $u_t = (\sin(x)u)_x$, $u(x, 0) = \sin(x)$. Approximate solution, $u_N(\cdot, t)$ and imaginary part of its Fourier coefficients, $\Im \hat{u}_k(t)$ at $t = 4.0$ **a** with $N = 64$; **b** with $N = 128$; **c** with $N = 512$

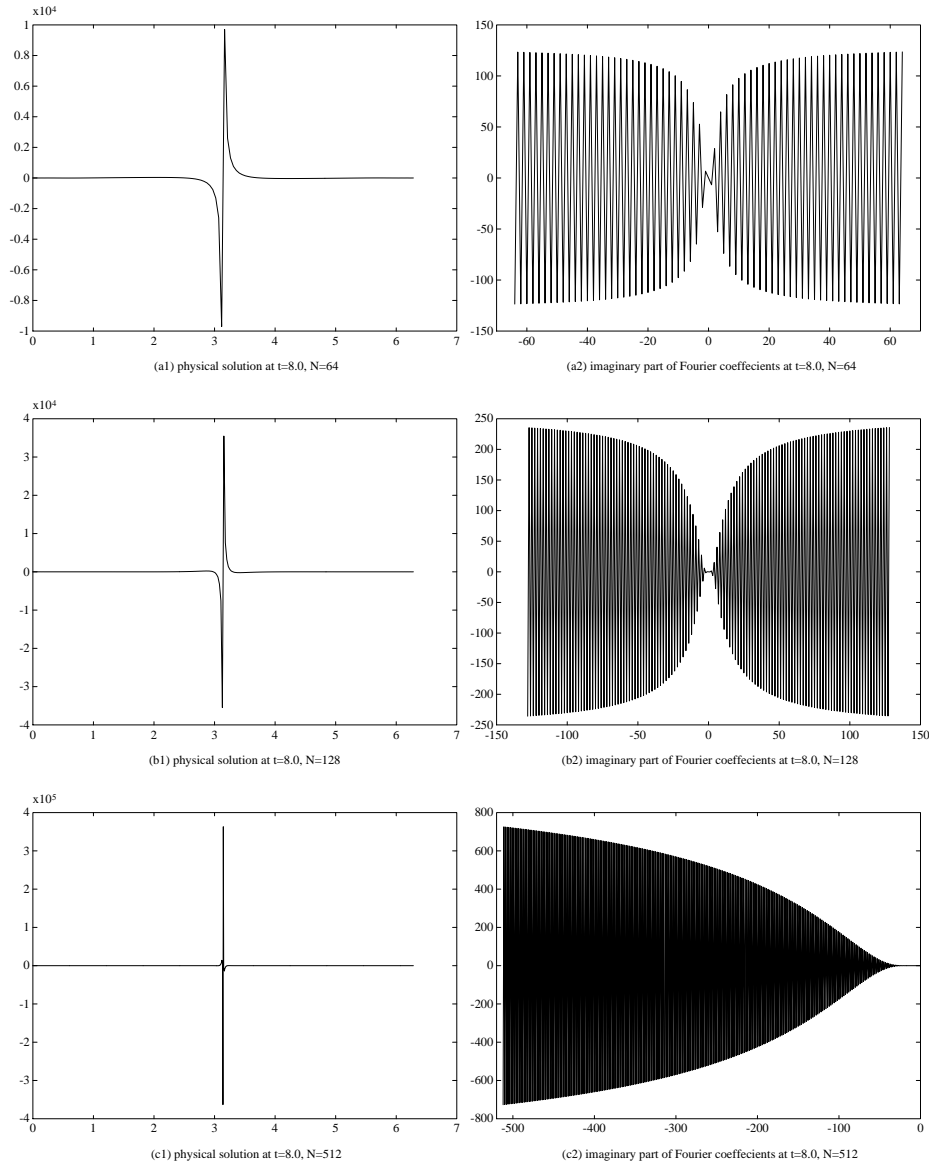


Fig. 9. a-c. Fourier solution of $u_t = (\sin(x)u)_x$, $u(x, 0) = \sin(x)$. Approximate solution, $u_N(\cdot, t)$, and imaginary part of its Fourier coefficients, $\Im m \hat{u}_k(t)$ at $t = 8.0$ **a** with $N = 64$; **b** with $N = 128$; **c** with $N = 512$

5. Weighted L^2 -stability revisited

In the previous sections we restricted our discussion on the stability of the Fourier method to what was claimed to be a prototype case (2.6) – a simple sinusoidal coefficient $q(x) = \sin(x)$. In this section we will try to substantiate this claim by extending our weighted stability analysis to include general coefficients, $q(x)$, belonging to one of the several large classes considered below.

As a first step we consider a general sinusoidal coefficient

$$(5.1)_p \quad \frac{\partial}{\partial t} u_N(x, t) = \frac{\partial}{\partial x} \psi_N[\sin(px)u_N(x, t)], \quad p = 1, 2, \dots$$

Though the technical details become more tedious, the ingredients are identical to those encountered before in the case $p = 1$; moreover, once weighted L^2 -stability is established this could be converted into an algebraically $O(N)$ -weak L^2 -stability along the lines of our discussion in Sects. 3 and 4.

As before, our starting point is the unitarily equivalent representation of (5.1)_p in the Fourier space, where

$$(5.2a) \quad \frac{d}{dt} \hat{u}_k(t) = \frac{k}{2} [\hat{u}_{k-p}(t) - \hat{u}_{k+p}(t)], \quad -N \leq k \leq N,$$

is augmented by the aliased boundary values

$$(5.2b) \quad \hat{u}_{\pm(N+k)}(t) = \hat{u}_{\mp(N-k+1)}(t) \equiv \bar{\hat{u}}_{\pm(N-k+1)}(t), \quad k = 1, 2, \dots, p.$$

Next, we form the p -adic blocks (for simplicity we assume that N is an integer multiple of p),

$$(5.3) \quad \hat{U}_k(t) := \begin{pmatrix} \hat{u}_{kp-p+1}(t) \\ \vdots \\ \hat{u}_{kp}(t) \end{pmatrix}, \quad -N_p \leq k \leq N_p := \frac{N}{p}.$$

The introduction of these p -adic blocks will not only greatly simplify the algebraic manipulations, but in retrospect it will be shown to capture the main features in this p -wave case.

Expressed in terms of these p -adic blocks, (5.2a) reads

$$(5.4a) \quad \frac{d}{dt} \hat{U}_k(t) = \frac{k}{2} \mathcal{L}_k [\hat{U}_{k-1}(t) - \hat{U}_{k+1}(t)], \quad -N_p \leq k \leq N_p,$$

augmented with the boundary conditions (5.2b),

$$(5.4b) \quad \hat{U}_{-(N_p+1)}(t) = \mathcal{H} \bar{\hat{U}}_{-N_p}(t), \quad \hat{U}_{N_p+1}(t) = \mathcal{H} \bar{\hat{U}}_{N_p}(t).$$

Here \mathcal{L}_k abbreviate the $p \times p$ diagonal matrix

$$\mathcal{L}_k := pI_p - \frac{1}{k} \begin{pmatrix} p-1 & & & \\ & \ddots & & \\ & & \ddots & \\ & & & 0 \end{pmatrix},$$

and \mathcal{H} denotes the anti-diagonal $p \times p$ unit matrix

$$\mathcal{H} := \begin{pmatrix} & & & 1 \\ & & \ddots & \\ & & & \\ 1 & & & \end{pmatrix}.$$

As before, we can decouple this system into its real and imaginary parts, $\hat{U}(t) = A(t) + B(t)$. The real part of the Fourier coefficients, $A_k(t) := \Re e \hat{U}_k(t) = (a_{kp-p+1}, \dots, a_{kp})$, satisfies

$$(5.5a) \quad \frac{d}{dt} A_k(t) = \frac{k}{2} \mathcal{L}_k [A_{k-1}(t) - A_{k+1}(t)], \quad -N_p \leq k \leq N_p,$$

$$(5.5b) \quad A_{-(N_p+1)}(t) = \mathcal{H} A_{-N_p}(t), \quad A_{N_p+1}(t) = \mathcal{H} A_{N_p}(t).$$

The imaginary part of the Fourier coefficients, $B_k(t) := \Im \hat{U}_k(t) = (b_{kp-p+1}, \dots, b_{kp})$, satisfies the same recurrence relations as before

$$(5.6a) \quad \frac{d}{dt} B_k(t) = \frac{k}{2} \mathcal{L}_k [B_{k-1}(t) - B_{k+1}(t)], \quad -N_p \leq k \leq N_p,$$

the only difference lies in the augmenting boundary conditions

$$(5.6b) \quad B_{-(N_p+1)}(t) = -\mathcal{H} B_{-N_p}(t), \quad B_{N_p+1}(t) = -\mathcal{H} B_{N_p}(t).$$

The boundary conditions (5.5b), (5.6b) suggest to introduce the local differences of the real part, $\rho_k^-(t) := \mathcal{H} A_k(t) - A_{k+1}(t)$, and the local averages of the imaginary part, $\rho_k^+(t) := \mathcal{H} B_k(t) + B_{k+1}(t)$. Differencing consecutive terms in (5.5a) while adding consecutive terms in (5.6a), we find (after taking into account the fact that \mathcal{L}_k and \mathcal{H} commute),

$$(5.7a) \quad \frac{d}{dt} \rho_k^\pm(t) = \frac{k}{2} \mathcal{L}_k \rho_{k-1}^\pm(t) - \frac{k+1}{2} \mathcal{L}_{k+1} \rho_{k+1}^\pm(t) \pm \frac{p}{2} \mathcal{H} \rho_k^\pm(t), \quad -N_p \leq k \leq N_p - 1.$$

As before, the motivation for considering this specific change of variables stems from the side conditions in (5.5b) and (5.6b), which are now translated into zero boundary values

$$(5.7b) \quad \rho_{-(N_p+1)}^\pm(t) = \rho_{N_p}^\pm(t) = 0.$$

Observe that (5.7a), (5.7b) amount to a fixed translation of *block antisymmetric* ODE systems for $\rho^-(t) := (\rho_{-N_p}^-(t), \dots, \rho_{N_p-1}^-(t))$ and $\rho^+(t) := (\rho_{-N_p}^+(t), \dots, \rho_{N_p-1}^+(t))$, that is, we have

$$\frac{d}{dt} \rho^\pm(t) = \frac{1}{2} (\pm p \mathcal{H} \otimes I + \mathcal{S}) \rho^\pm(t),$$

where \mathcal{S} denotes the block antisymmetric matrix

$$\mathcal{S} = \begin{bmatrix} 0 & S_{N_p-1} & 0 & \dots \\ -S_{N_p-1} & 0 & \ddots & 0 \\ 0 & \ddots & \ddots & S_1 \\ \vdots & 0 & -S_1 & 0 \end{bmatrix}$$

$$\oplus \begin{bmatrix} 0 & -S_1 & 0 & \dots \\ S_1 & 0 & \ddots & 0 \\ 0 & \ddots & \ddots & -S_{N_p-1} \\ \vdots & 0 & S_{N_p-1} & 0 \end{bmatrix}, \quad S_k = k\mathcal{D}_k.$$

This shows that upon change of variables, our problem is converted into an ODE governed by a fixed translation of an antisymmetric matrix. This implies that

Corollary 5.1. *The eigenvalues of the solution operator e^{DQt} associated with (5.1)_p, are of the form $e^{\lambda t}$ with $\operatorname{Re} \lambda \in \{0, \pm \frac{p}{2}\}$.*

Corollary 5.1 extends the result of Tal-Ezer [TE] for the case $p = 2$.

Next, since \mathcal{S} is antisymmetric we conclude the a priori L^2 bound

$$(5.8) \quad \|\rho^\pm(t)\| \leq e^{\pm pt/2} \|\rho^\pm(0)\|.$$

To interpret this in terms of the original real and imaginary variables we shall need to use the $N \times N$ Jordan-like blocks

$$J_{\pm, \mathcal{H}} := \begin{bmatrix} \mathcal{H} & \pm I_p & \dots & 0 \\ 0 & \mathcal{H} & \ddots & \vdots \\ \vdots & & \ddots & \pm I_p \\ 0 & \dots & 0 & \mathcal{H} \end{bmatrix}.$$

Assume temporarily that the initial conditions have zero average, (2.13), so that $a_0(t) \equiv 0$. Then A_0 and A_1 are related through $A_0 = N\mathcal{H}A_1$, where N is the canonical $p \times p$ "north" nilpotent matrix, $N := J_+ - I$. This enables us to invert the relation between the local differences, $\rho^-(t)$ and the 'punctured' vector of their real predecessors, $\tilde{A}(t) := (A_{-N_p}(t), \dots, A_{-1}(t), A_1(t), \dots, A_{N_p}(t))$,

$$\rho^-(t) = T_- \tilde{A}(t).$$

Here the transformation matrix T_- is given in terms of J_- , $J_{-, \mathcal{H}}$ and their transpose

$$T_- = \left[\begin{array}{ccc|ccc} \mathcal{H} & -\mathbf{I} & & & & \\ & \ddots & \ddots & & & \\ & & \ddots & & & \\ & & & -\mathbf{I} & & \\ & & & \mathcal{H} & -N\mathcal{H} & \\ \hline & & & -J_-^t & & \\ & & & \mathcal{H} & -\mathbf{I} & \\ & & & & \ddots & \ddots \\ & & & & & \mathcal{H} & -\mathbf{I} \end{array} \right].$$

The last equality together with (5.8) give us the weighted stability of the 'punctured' real part, $\|\tilde{A}(t)\|_{T_-^t T_-} \leq e^{-pt/2} \|\tilde{A}(0)\|_{T_-^t T_-}$. A similar treatment applied to the imaginary part yields $\|\tilde{B}(t)\|_{T_+^t T_+} \leq e^{pt/2} \|\tilde{B}(0)\|_{T_+^t T_+}$. Let us state the final result.

Theorem 5.2. *Let $u_N(t) \equiv u_N(\cdot, t)$ denote the solution of the Fourier method*

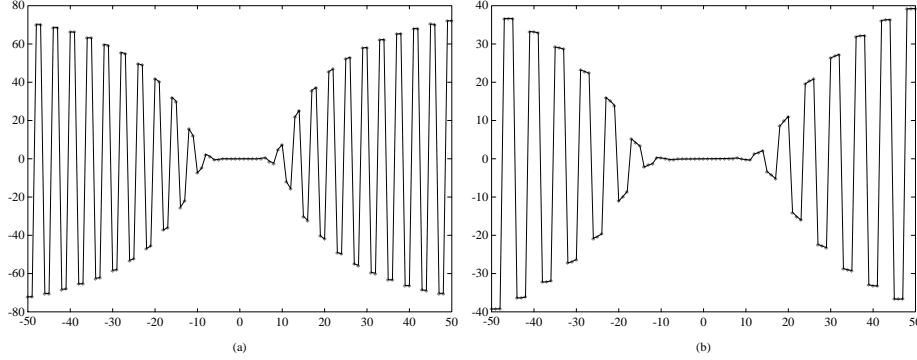


Fig. 10. a,b. Fourier Solution of $u_t = (\sin(px)u)_x$, $\hat{u}_k(0) = \sin(\xi_k)$. Imaginary part of Fourier coefficients, $\hat{u}_k(t)$, computed with $N = 50$ and $\Delta t = 0.004$ at **a** $t = 1.0$ ($p = 2$); **b** $t = 0.5$ ($p = 3$)

$$(5.9) \quad \frac{\partial}{\partial t} u_N(x, t) = \frac{\partial}{\partial x} \psi_N [\sin(px)u_N(x, t)].$$

Then there exists a constant, $C(t)$, such that the following weighted L^2 -stability estimate holds

$$(5.10) \quad |||u_N(t)|||_H \leq C(t) |||u_N(0)|||_H.$$

Here $|||u_N(t)|||_H$ denotes the weighted L^2 -norm

$$|||u_N(t)|||_H := \|\Re \hat{U}(t) \oplus \Im \hat{U}(t)\|_H,$$

where the weighting matrix $H := H_- \oplus H_+ > 0$ is given in terms of $J_{\pm, \mathcal{L}}$, J_{\pm} and their transpose.

As before, we can now proceed in two complementing directions. On the one hand, the weighted L^2 -stability stated in Theorem 5.2 together with the growth of $\kappa(T_{\pm})$ prove the algebraic L^2 -stability of the Fourier method. On the other hand, by repeating our previous arguments for the special case $p = 1$ we can trace the aliasing phenomenon as being responsible for the same weak L^2 -instability we had before. Indeed, the usual energy method shows the L^2 -stability of the real part in (5.5a), (5.5b), but as before it fails for the imaginary part, due to the judicious minus sign on the right of the aliasing boundary conditions (5.6b). The weak instability of the imaginary part manifests itself in terms of the modulated wave, $V_k(t) = (-1)^k B_k(t)$, which experiences a linear high-frequencies growth due to the augmenting *inflow-dependent* boundary conditions.

Figure 10 demonstrates this high-frequency instability in two prototype cases of $p = 2$ and $p = 3$. Observe that in both cases, it is the corresponding p -adic block which experiences the unstable binary oscillations, in complete agreement with our analysis.

Remark. It is easy to detect one set of unstable modes, at least for odd p 's. Indeed, if we set $b_k(t) = \Im \hat{u}_{kp + \frac{p+1}{2}}(t)$, then (5.2a) gives us

$$\frac{d}{dt} b_k(t) = \frac{pk}{2} [b_{k+1}(t) - b_{k-1}(t)], \quad -N_p \leq k \leq N_p := \frac{N}{p} + \frac{1-p}{2},$$

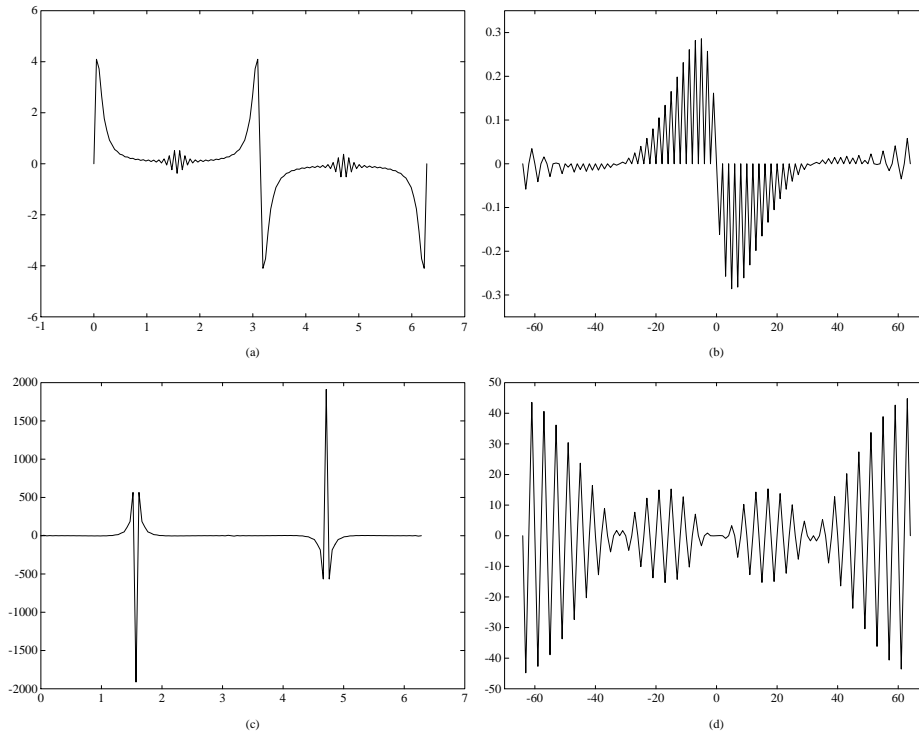


Fig. 11. a–d. Fourier Solution of $u_t = (\sin(2x)u)_x$, $u(x, 0) = \sin(x)$. Computed solution, $u_N(\cdot, t)$, and imaginary part, $\Im \hat{u}_k(t)$, with even number of $2N = 128$ modes **a** $u_N(\cdot, t)$ at $t = 1.2$; **b** $\Im \hat{u}_k(t)$ at $t = 1.2$; **c** $u_N(\cdot, t)$ at $t = 3.0$; **d** $\Im \hat{u}_k(t)$ at $t = 3.0$

complemented by the unstable aliasing reflection conditions (5.2b), $b_{\pm(N_p+1)}(t) = -b_{\pm N_p}(t)$.

We are now in a position to extend our stability analysis of the Fourier method in several directions. Let us briefly indicate few possible generalizations.

1. *Even number of gridpoints.* We can now treat the Fourier method based on an even number of $2N$ gridpoints, $x_\nu = \frac{\nu\pi}{N}$, $\nu = 0, 1, \dots, 2N - 1$. Let us consider for example the case $p = 2$ quoted in Table 3.2,

$$\frac{\partial}{\partial t} u_N(x, t) = \frac{\partial}{\partial x} \psi_N[\sin(2x)u_N(x, t)].$$

Expressed in terms of its Fourier coefficients, this approximation reads

$$\frac{d}{dt} \hat{u}_k(t) = \frac{k}{2} [\hat{u}_{k-2}(t) - \hat{u}_{k+2}(t)], \quad -N \leq k \leq N.$$

Observe that in the even case the corresponding Fourier interpolant is given by⁵, e.g. [GO],

⁵ As usual, we let the first (and second) primes indicate halving the first (and last) terms under summation.

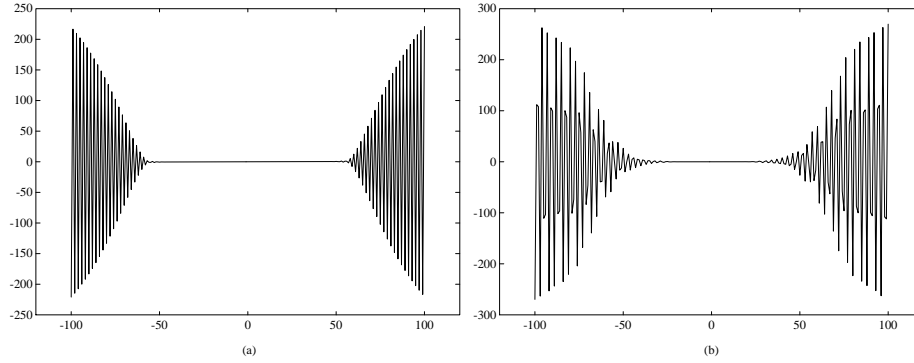


Fig. 12. a,b. Fourier Solution of $u_t = ((\sin(x) + \hat{q}_2 \sin(2x))u)_x$ at $t = 1$. Imaginary part of Fourier coefficients $\hat{u}_k(t)$ with $N = 100$ and **a** $\Delta t = 0.002$; $\hat{q}_2 = 0.2$; **b** $\Delta t = 0.0025$, $\hat{q}_2 = 1/1.14159$

$$\sum_{k=-N}^N \hat{u}_k(t) e^{ikx}.$$

It contains the correct number of $2N$ waves because – as we have noted earlier in (3.22), the last mode is necessarily ‘silent’, $b_{\pm N}(t) \equiv 0$. This implies that one-part of the imaginary components, namely, $\{\text{Im} \hat{u}_{2k}\}_{0 \leq k \leq N/2}$, is L^2 -stable. However, the odd-indexed imaginary components, $b_k(t) := \text{Im} \hat{u}_{2k-1}(t)$, satisfy

$$(5.11a) \quad \frac{d}{dt} b_k(t) = \frac{2k-1}{2} [b_{k+1}(t) - b_{k-1}(t)], \quad 1 \leq k \leq n := \frac{N}{2}$$

and augmented with the *unstable* inflow-dependent boundary conditions

$$(5.11b) \quad b_{n+1}(t) = -b_n(t).$$

Due to this decoupling, one is led to the same L^2 -growth of order $O(N)$, encountered before in (2.10a)-(2.10b). This even-odd decoupling in the Fourier space reflects the decoupling between the even and odd gridvalues on the physical side. Similarly, we can decouple at least one set unstable modes for the Fourier approximation of (5.1)_p. Figure 10 demonstrates this weak instability (due to lack of resolution), analogous to the results with odd number of modes in Figs. 5–9.

2. More simple wave coefficients. So far we considered simple sinusoidal coefficients. We consider the Fourier method based on even number of $2N$ gridpoints, and assume without loss of generality, that N is an integer multiple of the fixed wave number, $m = m_p := \frac{N}{2^p}$. Then the grid translation, $x_\nu \rightarrow x_{\nu+m}$ implies that $\sin(px_{\nu+m}) = \cos(px_\nu)$, which in turn converts our stability analysis of the sinusoidal problem (5.1)_p into the corresponding cosinusoidal problem,

$$(5.12)_p \quad \frac{\partial}{\partial t} u_N(x, t) = \frac{\partial}{\partial x} \psi_N[\cos(px)u_N(x, t)], \quad p = 1, 2, \dots$$

It should be noted that the real components are no longer stable in this case.

3. Combination of simple waves. We now consider more general variable coefficients of the form,

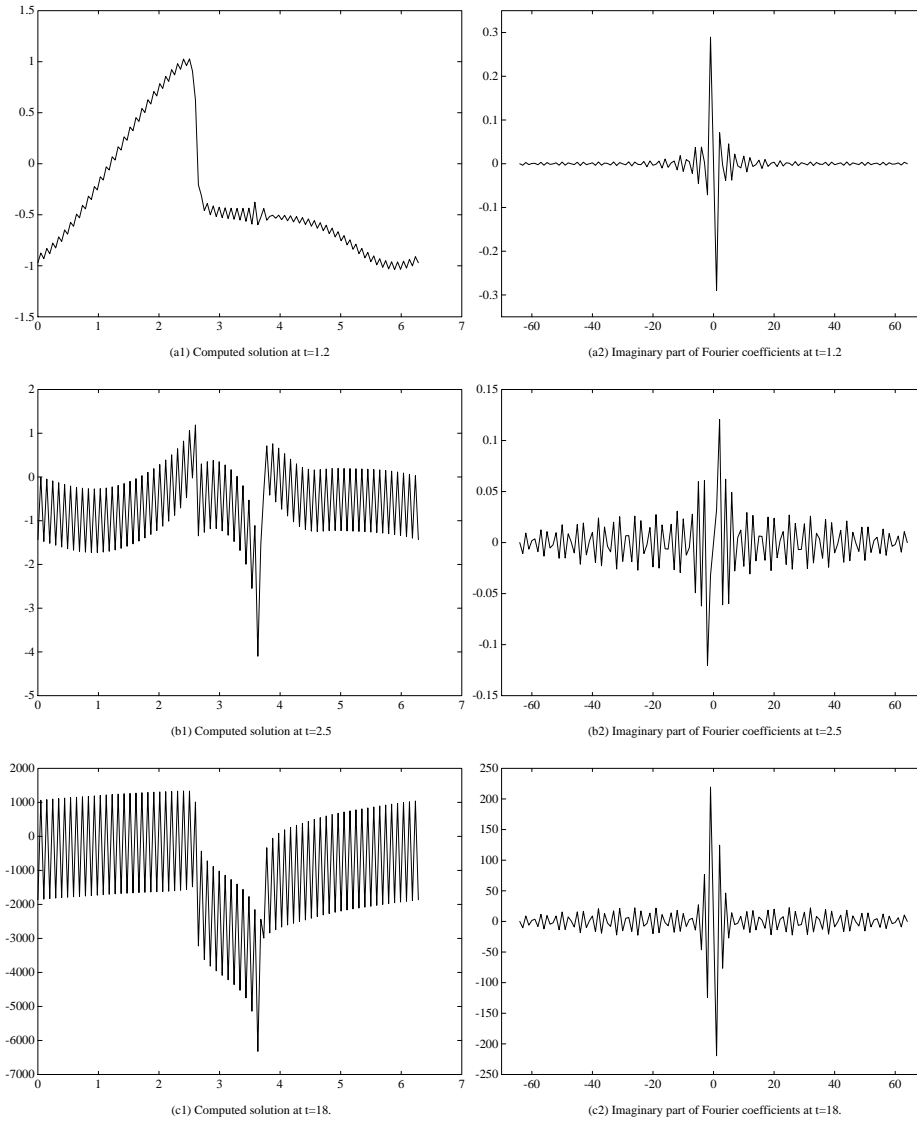


Fig. 13. a–c. Fourier solution of $u_t + q(x)u_x = 0$, $q(x) = 1 - 2e^{-10 \sin(\frac{x-\pi}{2})^2}$, $u(x, 0) = \sin(x)$. Computed solution, $u_N(\cdot, t)$, and imaginary part, $\text{Im}\hat{u}_k(t)$, with even number of $2N = 128$ modes at **a** $t = 1.2$; **b** $t = 2.5$; **c** $t = 18$

$$(5.12) \quad \frac{\partial}{\partial t} u_N(x, t) = \frac{\partial}{\partial x} \psi_N[q(x)u_N(x, t)], \quad q(x) = \sum_p \hat{q}_p \sin(px).$$

The detailed stability analysis in this case becomes more complicated. Unfortunately, one cannot adopt a straightforward 'splitting argument' in this case. Though each simple p -component of $q(x)$ is by itself weighted L^2 -stable, yet each makes use of different p -dependent weighting matrices. Instead one has to consider the behavior of an appropriate combination of the various p -adic blocks, along the lines of the proof of Theorem 5.2.

We shall confine ourselves to show at least one set of unstable modes. As before, we seek the behavior of an underlying modulated wave associated with the imaginary part of (5.12). Expressed in terms of $v_k(t) = (-1)^k \Im \hat{u}_k(t)$, the imaginary part of (5.12) reads

$$(5.13a) \quad \frac{d}{dt} v_k(t) = \frac{k}{2} \sum_p (-1)^p \hat{q}_p [v_{k+p}(t) - v_{k-p}(t)],$$

augmented by the boundary conditions

$$(5.13b) \quad v_{N+k}(t) = v_{N-k+1}(t), \quad k = 1, 2, \dots, p.$$

Observing that (5.13a) is consistent with

$$\frac{\partial}{\partial t} v(\xi, t) = -C_q \xi \frac{\partial}{\partial \xi} v(\xi, t), \quad C_q := \sum_p (-1)^p p \hat{q}_p < \infty,$$

we conclude that

Corollary 5.3. (Weak L^2 -instability.) *The Fourier method (5.12) is weakly unstable if either $\sum_p (-1)^p p \hat{q}_p < 0$ or $\sum_p p \hat{q}_p < 0$.*

In the first case, the imaginary components are governed by the unstable *inflow-dependent* boundary conditions (5.13b); in the second case, the instability shows in the corresponding real part. Note that $\sum_p (\pm 1)^p p \hat{q}_p < 0$ means that $q(x)$ decreases monotonically through a simple zero at either $x = \pi$ or $x = 0$.

Figure 12 shows the unstable behavior with a combination of two sinusoidal waves. Observe that two types of unstable modes are superimposed one on top of the other. The detailed information of this superposition is encoded in the corresponding initial-boundary value problem (5.13a), (5.13b), which in this case involves a 5-point stencil. Figure 13 demonstrates the increased complexity of this weakly unstable behavior with more general coefficients.

Acknowledgements. The first author (J. G) was supported by an NSF Presidential Young Investigator award and a grant from the ONR. The second author (T. H) was supported by a Sloan Foundation Research Fellowship, N.S.F. Grant No. DMS-9003202, and in part by A.F.O.S.R. under grant AFOSR-90-0090. He also wishes to thank the I.A.S. for its hospitality and the support under N.S.F. Grant No. DMS-9100383 during his visit to the I.A.S. from 9/1991 to 5/1992. The third author (E. T) was supported in part by ONR Grant #N00014-91-J-1076 while at University of S. Carolina, by NSF Grant #DMS 91-03104 while visiting UCLA, and by the basic Research Foundation, Israel Academy of Sciences and Humanities.

References

- [AGT] Abarbanel, S., Gottlieb, D., Tadmor, E. (1986): Spectral methods for discontinuous problems. In: K.W. Morton and M.J. Baines, eds., Numerical Analysis for Fluid Dynamics II, pp. 129–153. Oxford University Press
- [B] Boyd, J. (1989): Chebyshev & Fourier Spectral Methods. In: C.A. Brebbia, S.A. Orszag, eds., Lecture Notes in Engineering **49**, Springer, Berlin Heidelberg New York
- [CHQZ] Canuto, C., Hussaini, M.Y., Quarteroni, A., Zang, T. (1988): Spectral Methods in Fluid Dynamics. Springer, Berlin Heidelberg New York
- [Fo] Fornberg, B. (1975): On a Fourier method for the integration of Hyperbolic equations. SINUM **12**, 509–528
- [Fu] Funaro, D. (1992): Polynomial Approximation of Differential Equations. Lecture Notes in Physics **8**, Springer, Berlin Heidelberg New York
- [GKS] Gustafsson, B., Kreiss H.-O., Sundström, A. (1972): Stability theory of difference approximations for mixed initial-boundary value problems. II. Math. Comput. **26**, 649–686
- [GO] Gottlieb D., Orszag, S.A. (1977): Numerical Analysis of Spectral Methods: Theory and Applications. CBMS-NSF Regional Conference Series in Applied Mathematics **26**, Society for Industrial and Applied Mathematics, Philadelphia
- [GTa] Gottlieb D., Tadmor, E. (1985): Recovering pointwise values of discontinuous data with spectral accuracy. In: E.M. Murman and S.S. Abarbanel eds., Progress and Supercomputing in Computational Fluid Dynamics. Progress in Scientific Computing **6**, pp. 357–375, Birkhauser, Boston
- [GTu] Gottlieb D., Turkel, E. (1981): Spectral methods for time dependent partial differential equations. Lecture Notes in Mathematics **1127**, pp. 115–155, Springer, Berlin Heidelberg New York
- [GOT] Gottlieb, D., Turkel E., Orszag, S.A. (1981): Stability of Pseudospectral and finite-difference methods for variable coefficients problems. Math. Comput. **37**, 293–305
- [KL] Kreiss, H.-O., Lundquist, E. (1968): On difference approximations with wrong boundary conditions. Math. Comput. **22**, 1–12
- [KO1] Kreiss, H.-O., Olinger, J. (1972): Comparison of accurate methods for the integration of hyperbolic equations. Tellus **27**, 199–215
- [KO2] Kreiss H.-O., Olinger, J. (1979): Stability of the Fourier method. SINUM **16**, 421–433
- [MMO] Majda, A., McDonough J., Osher, S. (1978): The Fourier method for nonsmooth initial data. Math. Comput. **30**, 1041–1081
- [Or1] Orszag, S.A. (1971): Numerical simulation of incompressible flows within simple boundaries: accuracy. J. Fluid Mech. **49**, 75–112
- [Or2] Orszag, S.A. (1972): Comparison of Pseudospectral and Spectral approximations Stud. Appl. Math. **51**, 253–259
- [Os] Osher, S. (1969): On systems of difference equations with wrong boundary conditions. Math. Comput. **23**, 567–572
- [RM] Richtmyer R.D., Morton, K.W. (1967): Difference Methods for Initial Value Problems. Interscience, New York
- [Ta1] Tadmor, E. (1981): The unconditional instability of inflow-dependent boundary conditions in difference approximations to hyperbolic systems. Math. Comput. **41**, 309–319
- [Ta2] Tadmor, C. (1987): Stability analysis of finite-difference, pseudospectral and Fourier-Galerkin approximations for time-dependent problems. SIAM Review **29**, 525–555
- [Ta3] Tadmor, E. (1989): Convergence of spectral methods for nonlinear conservation laws. SINUM **26**, 30–44
- [Ta4] Tadmor, E. (1990): Spectral Methods for Time Dependent Problems. Internal ICASE Interim Report No. 14. Lecture Notes for the Nordic Summerschool on Numerical Methods in Fluid Dynamics, Sydoster, Sweden, NASA Langley Research Center, Hampton, VA
- [TE] Tal-Ezer, H. (1985): The eigenvalues of the Pseudospectral Fourier approximation to the operator $\sin(2x)\frac{\partial}{\partial x}$, ICASE Report No. 85-8. NASA Langley Research Center, Hampton, VA
- [Tr] Trefethen, L.N. (1984): Instability of difference models for hyperbolic initial boundary value problems. Comm. Pure Appl. Math. **37**, 329–367